ARTICLE OPEN

Check for updates

Multimodal beneficial effects of BNN27, a nerve growth factor synthetic mimetic, in the 5xFAD mouse model of Alzheimer's disease

Maria Kokkali[1,2,6], Kanelina Karali[1,2,6], Evangelia Thanou[3], Maria Anna Papadopoulou[1,2], Ioanna Zota[1,2], Alexandros Tsimpolis[1,2], Paschalis Efstathopoulos[1], Theodora Calogeropoulou[4], Ka Wan Li[3], Kyriaki Sidiropoulou[2,5], Achille Gravanis[1,2] and Ioannis Charalampopoulos[1,2]✉

Alzheimer's Disease (AD) is an incurable and debilitating progressive, neurodegenerative disorder which is the leading cause of dementia worldwide. Neuropathologically, AD is characterized by the accumulation of Aβ amyloid plaques in the microenvironment of brain cells and neurovascular walls, chronic neuroinflammation, resulting in neuronal and synaptic loss, myelin and axonal failure, as well as significant reduction in adult hippocampal neurogenesis. The hippocampal formation is particularly vulnerable to this degenerative process, due to early dysfunction of the cholinergic circuit. Neurotrophic factors consist major regulatory molecules and their decline in AD is considered as an important cause of disease onset and progression. Novel pharmacological approaches are targeting the downstream pathways controlled by neurotrophins, such as nerve growth factor (NGF) receptors, TrkA and $p75^{NTR}$, which enhance hippocampal neurogenic capacity and neuroprotective mechanisms, and potentially counteract the neurotoxic effects of amyloid deposition. BNN27 is a non-toxic, newly developed 17-spiro-steroid analog, penetrating the blood-brain-barrier (BBB) and mimicking the neuroprotective effects of NGF, acting as selective activator of its receptors, both TrkA and p75NTR, thus promoting survival of various neuronal cell types. Our present research aims at determining whether and which aspects of the AD-related pathology, BNN27 is able to alleviate, exploring the cellular and molecular AD components and link these changes with improvements in the cognitive performance of an animal AD model, the 5xFAD mice. Our results clearly indicate that BNN27 administration significantly reduced amyloid-β load in whole brain of the animals, enhanced adult hippocampal neurogenesis, restored cholinergic function and synaptogenesis, reducing inflammatory activation and leading to significant restoration of cognitive functions. BNN27 may represent a new lead multimodal molecule with neuroprotective, neurogenic and anti-neuroinflammatory actions for developing druggable anti-Alzheimeric agents. Proteomics data are available via ProteomeXchange with the identifier PXD044699.

Molecular Psychiatry; https://doi.org/10.1038/s41380-024-02833-w

INTRODUCTION

Alzheimer's Disease (AD) is a devastating neurological disease, consisting the most common cause of dementia. The number of people living with dementia is estimated to reach more than 150 million cases in 2050, with AD contributing to 60–80% of these patients [1]. A growing number of causes for AD and the multiple risk factors that are involved in its pathogenesis have been attributed both in familial and autosomal-dominant forms of AD, and can be caused by several mutations in the Amyloid-beta Protein Precursor (APP), presenilin 1 (PS1) and presenilin 2 (PS2) genes [2]. The disease is a neurodegenerative disorder characterized by progressive neuronal loss, resulting in brain atrophy and cognitive decline with no effective treatment so far. Its neuropathological hallmarks are the accumulation of amyloid-β (Aβ) plaques especially in the frontal, temporal and parietal cortices, the hippocampus and the cholinergic nuclei of the basal forebrain (ChBF), as well as the intra-neuronal neurofibrillary tangles containing tau protein [3–6]. In particular, the cholinergic system consists the earliest affected and most vulnerable region to Aβ deposition [7], and thus it was targeted as a primary therapeutic intervention [4, 8, 9]. However, AD is also featuring other pathologies such as the loss of synapses, which correlates with mental decline and white matter attenuation [10], observed even before any clinical symptoms [11], induction of inflammatory responses [12, 13] and demyelination [14, 15]. Even more recently, a growing number of studies have introduced the role of adult hippocampal neurogenesis as an important endogenous function that is significantly affected during AD progression, even in the

[1]Department of Pharmacology, School of Medicine, University of Crete, Heraklion 71003, Greece. [2]Institute of Molecular Biology and Biotechnology, Foundation for Research and Technology–Hellas, Heraklion 71003, Greece. [3]Department of Molecular and Cellular Neurobiology, Center for Neurogenomics & Cognitive Research, Neuroscience Campus Amsterdam, VU University, Amsterdam, The Netherlands. [4]Institute of Chemical Biology, National Hellenic Research Foundation, 11635 Athens, Greece. [5]Department of Biology, School of Sciences and Engineering, University of Crete, Heraklion 71003, Greece. [6]These authors contributed equally: Maria Kokkali, Kanelina Karali. ✉email: charalampn@uoc.gr

Received: 21 January 2024 Revised: 5 November 2024 Accepted: 6 November 2024
Published online: 25 November 2024

human brain [16, 17], and thus, it could potentially constitute a novel therapeutic target [18].

Recently approved drugs for AD have not shown robust safety, with side effects including meningoencephalitis, toxicity, and amyloid-related imaging abnormalities (ARIA), such as brain edema, sulcal effusion, and hemorrhagic hemosiderin deposits [19]. The majority of drugs tested in clinical trials have been immunotherapy-based monoclonal antibodies (mAbs) targeting a single protein, mainly amyloid, with a failure rate approaching 100% [20]. A recent breakthrough in amyloid therapeutics is aducanumab, marketed as Aduhelm, a synthetic monoclonal antibody targeting amyloid aggregates in both oligomeric and fibrillar forms. However, its efficacy is questionable, as the drug was approved solely for its ability to reduce amyloid, without significant symptomatic benefits for patients [21]. More recently, the FDA approved lecanemab, another amyloid immunotherapy targeting soluble aggregated amyloid protofibrils. Although the 12-month primary endpoints were not met across doses in Phase II, new trials indicate a 27% reduction in cognitive decline after 18 months. This is currently the most promising data from any Alzheimer's disease trial [22]. Given the lack of success so far of the Aβ targeting drugs and the complicated pathophysiology of AD, pharmacological strategies that may simultaneously affect multiple AD-related cellular mechanisms are more likely to be successful.

A novel class of such therapeutic approach is the neurotrophins and their receptors, which activate pathways highly important for adult neural tissue maintenance and regeneration while they have been closely associated to AD pathogenesis. Neurotrophin molecules are secreted polypeptidic growth factors, namely NGF, BDNF and NT3/4, whose main function is to induce neuronal survival and regeneration [23], operating through selective binding to two classes of membrane receptors, the high affinity Trk receptors and the low affinity p75 pan-neurotrophin receptor [24]. These receptors can function independently or interact physically and functionally with each other, in ways that can change the signaling characteristics of each receptor, ranging from pro-survival and neurogenic effects (mainly mediated by Trk receptors) up to cell death signals (upon activation of the p75NTR death receptor) [25, 26]. The prototype neurotrophin, NGF (described by the pioneering work of Levi-Montalcini & Booker at 1960) [27], binds to its cognate tropomyosin-related kinase A (TrkA) receptor and with lower affinity to p75 pan-neurotrophin receptor (p75NTR) [24]. A plethora of studies have demonstrated that NGF deprivation results in AD-like pathologies, such as Aβ accumulation/deposition, tau hyperphosphorylation and synaptic dysfunction in mice, while NGF treatment can ameliorate the changes of amyloid pathologies and inhibit memory impairment in AD animal models [28], being also tested in clinical trials [29, 30]. Both NGF receptors, TrkA and p75NTR, are strongly implicated in AD onset and progression [31]. Specifically, their expression levels in hippocampal formation are altered during AD [32], especially at the cholinergic neurons that express both receptors [33], with ablation of TrkA in basal forebrain to induce cholinergic circuitry dysfunction [34], and p75NTR deletion to rescue synaptic loss [35], amyloid-β plaque deposition and eventually restore cognitive impairments [36], in mouse models of AD. Moreover, numerous studies have shown that p75NTR mediates neurotoxic and pro-inflammatory Aβ signals [37–40], possessing a key role in AD exacerbation. Recently, the results of a Phase 2a clinical trial for a p75NTR modulator were published [41], further indicating receptor's significance in AD therapeutics.

All the aforementioned neurotrophin effects in brain function and repair have highlighted these molecules and their receptors as promising therapeutic candidates for treatment of neurodegenerative conditions, especially AD. However, the therapeutic usefulness of endogenous neurotrophins is compromised by their polypeptide nature and their restricted penetrance to the blood-brain barrier (BBB). Attempts to bypass these limitations, such as intracerebroventricularly infusion [42] or intranasal delivery of BDNF and NGF [43, 44], have shown limited beneficial effects in clinical trials and only a small amount of the applied drug finally reaches the CNS with intranasal delivery [29, 30].

Alternatively to neurotrophin use as drugs, recent efforts target on developing small molecules, with favorable pharmacological properties, acting as neurotrophin mimetics, meaning selectively activate one or more neurotrophin receptors. Several research groups have designed and tested such small neurotrophin analogs in AD, acting as agonists or antagonists of Trk and p75NTR receptors (reviewed in Longo & Massa, 2013 for all neurodegenerative diseases and in Kazim & Iqbal, 2016 for AD) [45, 46]. Briefly, ultrasound delivery of a TrkA agonist protects cholinergic neurons [47], another small-sized, non-peptidic TrkA agonist resembles NGF actions [48] and gambogic amide induce neuronal survival acting as TrkA activator [49], while modulation of p75NTR blocks cholinergic degeneration and prevents cognitive decline in mouse models of AD [50, 51]. Compound LM11A-31, proprietary of Dr Longo group, has been found to inhibit degenerative signaling in multiple in vitro and in vivo AD models and is currently undergoing testing in a human phase 2a trial in AD (NCT03069014) [41].

Our previous work has shown that the neurosteroid Dehydroepiandrosterone (DHEA) exerts part of its anti-apoptotic [52] and neurotrophic properties through activation of both NGF receptors [53]. In addition, we have developed and patented synthetic C17-derivatives of DHEA (named BNNs) [54], shown to interact with NGF receptors, which are deprived of any harmful estrogenic or androgenic effects, in contrast to endogenous DHEA [55, 56]. BNN27, as the prototype member of these synthetic analogs for neurotrophins, has been extensively studied at the molecular level for its ability to selectively activate TrkA and p75NTR receptors, exerting strong neuroprotective effects mediated by the TrkA and p75NTR receptors in cell models of neurotoxicity and neurodegeneration [56] as well as in in vivo models of diabetic retinopathy [57], demyelination [58], apomorhine-induced cognitive decline [59] and spinal cord injury [60]. The effect of BNN27 in all aforementioned studies is exclusively mediated through TrkA and/or p75NTR receptors, since blocking of specific receptor in each case fully diminishes the neuroprotective effect of the compound. Moreover, in several in vivo studies, both intraperitoneal or eye-drop administration of the compound could penetrate the BBB and exert its effects on CNS [57, 60, 61], clearly indicating that the CNS levels of the compound are able to activate TrkA and p75 receptors (EC_{50} at the nanomolar level) [55, 56]. In the present study, we sought to investigate whether BNN27 could mimic in vivo NGF actions against the AD phenotype and attenuate the well described AD-related neuropathology of the 5xFAD mice. This well-described mouse model of AD overexpresses both mutant human amyloid precursor protein (APP) with the Swedish (K670N, M671L), Florida (I716V), and London (V717I) FAD mutations and human presenilin 1 with two FAD mutations, M146L and L286V [62]. BNN27 capsules were subcutaneously applied over 60 days (10mg/kg/day) in 1.5 months old 5xFAD mice and their wild type littermates (concentration levels of the compound have been detected in blood serum and brain, see also Tsika et al, 2021) [63]. Mice, aged 3.5 months after the completion of the steady release of the aforementioned capsules, were subsequently assessed for a possible improvement of the cognitive performance. BNN27 was able to improve cognitive performance in the 5xFAD mouse model as measured in spontaneous alternation test, that was used to justify hippocampal-dependent working memory amelioration. Remarkably, BNN27 in vivo treatment resulted in a considerable decrease of the Aβ plaque formation within the hippocampus, while it promoted neuronal regeneration by inducing proliferation of newborn cells in the Dentate Gyrus neurogenic niche of the 5xFAD animals. Given the promising in vivo results, we isolated

primary hippocampal neural stem cells at postnatal day 7 (P7 NSCs) and hippocampal neurons at embryonic day 17.5 (E17.5) and we examined in vitro the major molecular and cellular hallmarks of the disease (proliferation, apoptosis, astrogliosis) in the presence or absence of BNN27 and/or amyloid β (Aβ). Our in vitro findings further supported the neuroprotective phenotype observed in vivo. The downstream pathways through which these procedures are manifested and the potential beneficial role against the pro-inflammatory astrogliosis are justifying the neuroprotective phenotype observed in vivo. Finally, the quantitative proteomics results indicate that Aβ induces major changes that reflects the AD pathology in our mouse model hippocampus and BNN27 administration has global rescue effects on this Aβ induced negative impact.

Conclusively, the present in vivo study of BNN27 in the 5xFAD mice model of AD, as well as the comprehensive in vitro results in mature neurons/glia and stem cells, decipher the cellular and molecular mechanisms that BNN27 induce through the selective activation of TrkA and p75NTR receptors, proposing this small, BBB-permeable molecule as a novel therapeutic approach against neurodegenerative disorders.

MATERIALS AND METHODS

Animals

Adult, male, 5xFAD transgenic mice harboring the five familial Alzheimer's disease linked mutations (APP KM670/671NL (Swedish), APP I716V (Florida), APP V717I (London), PSEN1 M146L (A>C), PSEN1 L286V) were used in this study [62]. Original breeders were obtained from Jackson Laboratories and bred in-house on a C57Bl/6J background. For this study cohorts of young (1.5 months old) 5xFAD mice and aged-matched wild type C57Bl/6J littermates were used. The animals were group-housed (3–5 animals/cage) in climate-controlled conditions (30–50% humidity, 21 ± 2 °C, 12:12 h light/dark cycle) with ad libitum access to food and water. Animals were habituated to housing conditions for 1 week prior to the beginning of the experimental procedures. All procedures were performed under the approval of Veterinary Directorate of Prefecture of Heraklion (Crete) and carried out in compliance with Greek Government guidelines and the guidelines of FORTH ethics committee and were performed in accordance with approved protocols from the Federation of European Laboratory Animal Science Associations (FELASA) and Use of Laboratory animals [License number: EL91-BIOexp-02), Approval Code: 360667, Approval Date: 29/11/2021 (active for 3 years)].

BNN27 administration

BNN27 was administered using a Matrix-Driven Delivery (MDD) Pellet system as previously described [58]. BNN27 custom made pellets (Innovative Research of America, Sarasota, FL) comprised of a biodegradable matrix were subcutaneously implanted at the lateral side of the neck of 1.5 months old 5xFAD and wild type mice which allowed a 60-day release of 10 mg/kg/day BNN27 (18 mg in total, average weight of the animals ≈ 30g). Placebo pellets comprised of only the biodegradable matrix were also implanted as controls.

Behavioral testing

After the completion of the 60-day release, the 3.5 months old mice were habituated (1h every day for 1 week) in an enclosed apparatus in the shape of a T placed horizontally, called T-maze [Start alley, Goal arm (x2): 30 cm × 10 cm, wall height: 20 cm, central partition: extended 7 cm into start arm]. The T-maze was used to test hippocampal-dependent working memory retention. Before T-maze testing, mice were acclimated in the same room where the test would take place for 1 h (the mice were familiarized for 1 week with the experimenter). Mice were taken out of the cage and let freely to walk on the experimenter's loosely folded arms and hands for at least 10 min. The animals are started from the base of the T and allowed to choose one of the goal arms (placed in the T-maze facing the wall of the start arm). The rationale of the test is that, if two trials are given in quick succession, on the second trial the rodent tends to choose the arm not visited before, reflecting memory of the first choice. Between two successively trials, the guillotine door blocks the access to the central partition for 30 s so as for the mouse to familiarize with the surroundings. This is called 'spontaneous alternation'. Spontaneous alternation is very sensitive to dysfunction of the hippocampus, but other brain structures are also involved. Ten trials were given for each mouse to test the alternation capability. Each trial should be completed in under 2 min, if that is not the case the mouse is removed from the maze and reintroduced to the start arm abutting the central partition [64]. Behavioral tests were conducted between 8:00 am and 12:00 pm. A custom-made interface connected to the computer allowed us to video record each animal.

Tissue processing

After the completion of behavioral testing, the animals (n = 7–9 per group) were sacrificed. For adult neurogenesis analysis, a separate cohort of animals (n = 4 per group) that had not undergone behavioral testing and had been injected with (5-bromo-2′-deoxyuridine) BrdU (100mg/kg) 21 days prior to sacrifice were used. Animals were deeply anesthetized with 5% isoflurane (Iso-Vet, Biovet) in a mixture of 30% O_2 and 70% N_2O and trans-cardially perfused with 20 mL 0.9% heparinised saline. Brains were immediately extracted and bisected along the midline. One hemibrain was post-fixed for 24 h in 4% paraformaldehyde (Sigma-Aldrich, St. Louis, MO, USA) and serial sagittal 40 µm sections starting at lateral 2.40 ± 0.1 mm, according to Franklin and Paxinos (1997) [65] were cut using a vibratome (Hydrax V50, Zeiss, Germany). The brains for neurogenesis analysis were cut in coronal sections of 40 µm in the dorsoventral axis of hippocampus (from bregma −1.34 mm to −3.80). Sections were stored in cryoprotective medium (30% glycerol/30% ethylene glycol in phosphate buffer) at −20 °C for subsequent immunohistochemical analysis. The hippocampi were dissected from the other hemibrain, snap frozen in liquid nitrogen and stored at −80 °C for subsequent proteomic analysis.

Amyloid beta (Aβ) treatment

Aβ42 peptide was purchased from AnaSpec (San Jose, CA). Aβ42 oligomers and fibrils were prepared according to previously established protocols [66]. For oligomeric Aβ treatment, peptides were diluted in DMEM / F-12 or Neurobasal medium at the indicated concentrations and incubated at 37 °C for 24 h. Then, the solution was centrifuged at 14,000 rpm for 5 min and the supernatant was collected as oligomeric Aβ to treat the primary cultures [66].

Neural stem (NS)/precursors cells (PCs) cultures

The protocol we followed is described in detail in Efstathopoulos et al. (2015) [67]. The hippocampi of postnatal day 7 (P7) C57/BL6 mice were digested for 30 min in accutase solution (Sigma-Aldrich) at 37 °C. After mechanical dissociation, cells were plated at a density of 5×10^4 cells/ mL into uncoated T25 culture flasks in Dulbecco's Modified Eagle's Medium/Nutrient Mixture F-12 Ham (Sigma-Aldrich) supplemented with 1% B27 w/o Vitamin A (Invitrogen, Thermo Fisher Scientific, Waltham, MA, USA), L-glutamine 2 mM (Gibco, Thermo Fisher Scientific), D-glucose 0.6%, primocin 100 µg/ mL (Invivogen), in the presence of 20 ng/ mL FGF2 (R&D Systems, Minneapolis, MN, USA), 20 ng/ mL EGF (R&D) and heparin (2mg/ mL STEMCELL Technologies) and allowed to form neurospheres. Cells were passaged every 5th day by dissociating neurospheres into single cells with accutase (Sigma-Aldrich).

Hippocampal neuronal cultures

E17.5 primary hippocampal cell culture was performed as previously discussed [68]. Brains of C57/BL6 mice fetuses [embryonic day 17.5–18 (E17.5)] were dissected, the meninges, vascular tissue excess were removed under a stereoscope and the hippocampi were isolated. Hippocampi were transferred to a 15 mL tissue culture tube and the volume was adjusted to 5 mL with dissection medium [HBSS (10X) (14185-045, GIBCO), 0.1% D-(+)-Glucose solution (G8769, Sigma), 10mM HEPES Buffer Solution (1X, 15630080 GIBCO), 500 U/ mL Penicillin-Streptomycin (10,000 U/ mL, 15140122, Thermo Fischer Scientific)] supplemented with 2.5% Trypsin 10x. Hippocampi were mechanically dissociated by trituration with a Pasteur pipet (−15 times) followed by trituration (−15 times) with a reduced-bore Pasteur pipet. The cells were pelleted by centrifugation at 1000 x g for 5 min. Cells were taken up in 500 µl of Neurobasal medium, passed through a cell strainer and counted in a hemocytometer. Approximately 8 x 10^4 cells per well were plated on poly-D-lysine coated 24-well plates in DMEM/F-12 medium containing 10% fetal bovine serum (FBS, 10270 Thermo Fischer Scientific, South American Origin), 10 mM HEPES Buffer Solution (1X, 15630080 GIBCO), 500 U/mL Penicillin-

Streptomycin (10,000 U/ mL, 15140122, Thermo Fischer Scientific) and cultured at 37 C in 5% $C0_2$/95% air. After 2 h, the 'plating' medium described above was aspirated and cells were incubated in 'feeding' medium, thus Neurobasal medium containing B-27 (TM) plus supplement (50X) (A3582801, Thermo Fischer Scientific), GLUTAMAX I, 100X (3505006, Thermo Fischer Scientific), 10 mM HEPES Buffer Solution (1X, 15630080 GIBCO), 500 U/mL Penicillin-Streptomycin (10,000 U/mL, 15140122, Thermo Fischer Scientific). Medium was changed every 3–4 days.

Glial primary cultures

Cerebral cortices from P2-P4 C57BL/6 mice were dissected and mixed glial cultures were prepared. Pure astrocytic cultures were isolated and cultured as described in [69]. Briefly, at DIV 6–8, Ara-C 10 μM was added to the culture medium for 4 days. Culture medium was then changed to with fresh medium without Ara-C. Cultures were expanded the next day. Medium was replaced every 3 days. Astrocytic cultures were used after the 2nd passage when their purity was > 98%. Pure microglial cultures were prepared and cultured using a mild trypsinization protocol as described in Saura et al. (2003) [70]. Briefly, after preparation of the mixed glial cultures, medium was replaced every 5–7 days. At DIV 18–20, culture medium is replaced with fresh. After 48h, culture medium is collected and kept at 37 °C as conditioned culture medium. Cultures are then washed once with serum-free medium and then incubated with trypsin solution 1:4 in serum-free culture medium for 35–45 min inside the incubator until the astrocytic feeding layer is fully detached. Then, an equal volume of culture medium with serum is added and the medium with the detached cells is removed. The stored conditioned medium is then returned to the cultures. Microglial cells can be used experimentally the next day, when their purity is >98%. Microglia condition media (MCM) treatments in astrocytes were achieved by performing an initial 24 h-long treatment in microglia cultures. LPS was used at a concentration of 100 ng/mL, Aβ42 oligomers were used at a concentration of 10 μM and BNN27 at a concentration of 10^{-7} M. After 24 h, MCM was collected and transferred into naïve astrocytic cultures for 24 h.

Oligodendrocyte primary cultures

Primary mixed glial cell cultures were derived from the cortices of postnatal day 2 C57BL/6 mouse pups, following a modified protocol based on McCarthy and de Vellis (1980) and further adjustments by Tamashiro et al. (2012) and Bonetto et al. (2017) [58, 71, 72]. After removing the meninges, the cortices were minced and mechanically dissociated using 2.5% trypsin (Thermo-15090046). The cells were then cultured in 75 cm^2 flasks coated with poly-D-lysine (PDL, Sigma-Aldrich, 50 mg/ml) in DMEM (GlutamaxTM, 4.5 g/L D-Glucose, without Pyruvate (Gibco)), supplemented with 10% FBS (Biosera) and 1% penicillin/ streptomycin (Gibco), until a distinct glial cell layer developed. The culture medium was replaced twice a week. Upon reaching 90% confluence (around 10–12 days), microglial cells were isolated by shaking at 200 rpm for 1 h at 37 °C, followed by discarding the medium containing microglia and adding fresh medium. Oligodendrocyte precursor cells (OPCs) were then separated from the astrocytic layer by shaking vigorously (18 h at 230 rpm, 37 °C) and seeded onto PDL-coated 96-well plates at a density of 9×10^3 cells per well. These cells were maintained in DMEM (Thermo-61965026) supplemented with 1% N2 (Thermo-17502048), 100 ng/ml biotin (Sigma-Aldrich), 1% BSA-Free Fatty acids (Sigma-Aldrich), 60 μg/ml cysteine (Sigma-Aldrich), 1% P/S, 10 ng/ml FGF-2 (Peprotech), and 10 ng/ml PDGF-AA (Peprotech).

OPC maturation protocol

OPCs were cultured for 48 h in a proliferation medium containing 10 ng/ml FGF and 10 ng/ml PDGF-AA. They were then maintained in a differentiation medium supplemented with 40 ng/ml T3 (Sigma) and treated with 5 μM Amyloid-β (1–42) (AnaSpec) and 100 ng/ mL mouse NGF 2.5S (>95%) (100 μg/ mL, N-100, Alomone) for another 48 h. Stock solutions of Amyloid-β, NGF, and T3 were prepared in 1xPBS as per the manufacturer's instructions, and an equivalent volume of 1xPBS was used for control samples. Following treatment, the cells were fixed and stained for O4, a marker for immature oligodendrocytes. Hoechst (1:10000, H3570, Invitrogen, Waltham, MA, USA) was used to visualize cell nuclei. Images were captured using a Zeiss AXIO Vert A1 fluorescent microscope (Zeiss, Jena, Germany).

NS/PCs proliferation and survival assay, receptor inhibition

For the proliferation assay, at the end of the treatments of the primary hippocampal Neural Stem Cell (NSC) cultures, 10 mM BrdU was applied for 4 h to label all actively proliferating cells before they were fixed and stained against BrdU. Furthermore, for the inhibition observation experiments, cells were exposed for 24 h to 100 ng/ mL human BDNF (100 μg/ mL, B-250, Alomone) or 100 ng/ mL mouse NGF 2.5S (>95%) (100 μg/ mL, N-100, Alomone) or 100nM BNN27 dissolved in DMSO (A3672, APPLICHEM) in the presence or absence of 50 nM of panTrk inhibitor (50 μM AZD-1332, A-495, Alomone) or p75NTR inhibitor [Anti-p75 NGF Receptor antibody MC-192, ab6172, Abcam]. Conclusively, for the cell death or cytotoxicity detection and quantification of both NSC and neuronal cultures, cells were fixed and stained with in situ cell death detection labeling kit (terminal deoxynucleotidyl transferase dUTP nick end labeling (TUNEL, 11684795910, Roche, Basel, Switzerland) and Celltox Green Cytotoxicity Assay (G8742, Promega), respectively, according to the manufacturer's instructions.

Immunofluorescence

Free-floating sections or neural stem/precursor cells (NS/PCs), hippocampal neuronal cultures (attached in Poly-D-Lysine 0.1 mg/ mL w/ or w/o Laminin 10 mg/ mL were fixed with 4% paraformaldehyde solution for 10–15 min, washed with PBS (1X), PBSTx (Triton X-100, 0.1% in PBS) and blocked in 10% Normal Serum (specific to the species the 2ary Ab(s) is/are raised), 0.1% BSA in 0.3% Triton X-100 in PBS (PBSTx) for 1 h at room temperature before they were incubated with primary antibodies in blocking solution overnight at 4 °C. The day after sections or cells were washed twice with PBS and incubated with Alexa Fluor chromophore-conjugated secondary antibody (1:1000, Invitrogen) in 0.1% PBSTx for 1 h at room temperature. Finally, sections or cultured primary cells were washed twice again with PBS and incubated with HOESCHT, washed again thrice with PBS and mounted onto slides using VECTASHIELD® Vibrance™ Antifade Mounting Medium (VECTOR). For detection of BrdU-labeled nuclei, specimens have been previously incubated in 2N HCl at 37 °C for 30 min, followed by a 10 min rinse in 0.1 M sodium tetraborate pH 8.5 and two rinses with PBS before blocking step. Maximum intensity projection images of confocal z-stacks were obtained with Leica SP8 confocal microscope.

qRT-PCR

Total RNA from postnatal day 7 hippocampal NSCs was extracted using Nucleospin RNA (#740955.50, Macherey Nagel) according to the manufacturer's instructions and stored at −20 °C. RNA concentration and quality were determined using a Bioanalyzer (Agilent). PCR products were resolved on a 1.2% agarose gel. To generate cDNA, ≤5 μg of total RNA was used, utilizing the PrimeScript 1st strand cDNA synthesis kit (#61110A, TAKARA Clontech Cellartis). GAPDH was used as a normalization control. RT-PCR was performed for 40 cycles for all markers as follows: Holding Stage for 3 min at 95 °C, Cycling Stage for 3 s at 95 °C and 60 °C for 30 s, Melt Curve Stage for 15 s at 95 °C and 60 °C for 1min and finally extending at 95 °C for 15 s. Data collected from qRT-PCR were corrected for differences in RNA input using the reference gene GAPDH. All of the primers that were used had 90–105% efficiency. Primer sequences: mGAPDH (forward, 5' ATTGTCAGCAATGCATCCTG 3'; reverse, 5' ATGGACTGTGGTCATGAGCC 3'), mTrkA (forward, 5' AGAGTGGCCTCCGCTTTGT 3'; reverse, 5' CGCATTGGAGGACAGATTCA 3'), mTrkB (forward, 5' TGGACCACGCCAACTGACATT 3'; reverse, 5' GAATGTCTCGCCAACTTGAG 3'), mhTrkC (forward, 5' TGCAGTCCATCAACACTCACCAGA 3'; reverse, 5' TGTAGTGGGTGGGCTTGTTGAAGA 3'), mp75NTR (forward, 5' GACTAACCTAGGCCACCCAA 3'; reverse, 5'CAGACGTCGTTTCCAGATGT 3').

Total RNA from astrocytic cultures was extracted using TRIzol Reagent (Invitrogen) and cDNA synthesis was performed using the High-capacity cDNA Reverse Transcription kit (Thermo Scientific, 4368814). Quantitative RT-PCR was run using 1μl of cDNA and KAPA SYBR FAST (Roche, KK4601) following the instructions of the supplier and a cycling program of 20s at 950C followed by 40 cycles of 950C for 3s and 600C for 30s. After that, a melting curve of the amplified products was performed. Data collected from qRT-PCR were corrected for differences in RNA input using the reference gene Actin. All of the primers that were used had 90–105% efficiency. Primer sequences:

mActin (forward, GGAGATTACTGCTCTGGCTC; reverse, GGACTCATCGTACTCCTGCT), mGfap (forward, AGAAAGGTTGAATCGCTGGA; reverse, CGGCGATAGTCGTTAGCTTC), mSteap4 (forward, CCCGAATCGTGTCTTTCCTA; reverse, GGCCTGAGTAATGGTTGCAT), mSerpina3n (forward, CCTGGAGGATGTCCTTTCAA; reverse, TTATCAGGAAAGGCCGATTG), mAmigo2 (forward, GAGGCGACCATAATGTCGTT; reverse, GCATCCAACAGTCCGATTCT), mSrgn (forward, GCAAGGTTATCCTGCTCGGA; reverse, TGGGAGGGCCGATGTTATTG), mSerping1 (forward, ACAGCCCCCTCTGAATTCTT; reverse, GGATGCTCTCCAAGTTGCTC).

Western blot

Cells were harvested in PIERCE IP Lysis Buffer (87788, Thermo Fischer Scientific) and supplemented with protease (539131, Millipore) and phosphatase (524629, Millipore) inhibitors, after they were washed twice with PBS (1X) and stored in −20 °C. The protein concentration was estimated by the bicinchoninic acid method (BCA, 23227, Pierce) and 15 µg of total protein was loaded and run-on sodium dodecyl sulfate–PAGE (15-well, 8% Bis-Tris gel) at 120 V for 90 min, then transferred to a nitrocellulose membrane (0.45 µm, Amersham) at 300 mA for 180 min. The proteins were then transferred to a nitrocellulose membrane and blocked in a solution of 5% BSA and 0.1% Tween-20 in TBS (TBS-T) for 1 h followed by incubation with the primary antibody in blocking solution overnight at 4 °C. The next day, the membranes were washed three times in TBS-T and was subsequently incubated with the appropriate horseradish peroxidase-conjugated secondary antibody (1:5000, Millipore and Invitrogen) in blocking solution for 1 h. Finally, the membranes were washed again in TBS-T and incubated for detection with enhanced chemiluminescence substrate (34580, Pierce) and the immunoreactive bands were visualized by scanning with a Bio-Rad image analysis system. Then, relative protein expression was normalized to the control conditions in each experiment. Mean values were estimated from three different cultures.

Antibodies and reagents

The samples were incubated in the primary antibody diluted in phosphate buffer (PBS) with Triton X-100 0.1%. For immunohistochemistry and immunocytochemistry, the antibodies used were mouse anti- Aβ (6E10 clone, Covance, 1:500); rabbit anti-Doublecortin antibody (DCX, Abcam, 1:200); mouse anti-NeuN clone A60 (Sigma-Aldrich, 1:100); mouse anti-BrdU (MoBU-1. Clone, Thermo Fischer Scientific, 1:200); chicken anti-Glial Fibrillary Acidic protein (GFAP, Millipore, 1:1000); Synapsin I (1:200, Novus Biologicals); Synaptophysin (Sigma-Aldrich, 1:200); rabbit anti-Iba1 (Wako Chemicals, 1:500); rabbit anti-TrkA (Millipore, 1:500); rabbit anti-p75 (Promega, 1:500); mouse anti-Choline Acetyltransferase (CL3173) (ChAT, Novus Biologicals, 1:2000); rat Anti-Myelin Basic Protein antibody (MBP, clone 12, Millipore, 1:200; chicken anti-Nestin (Novus Biologicals, 1:1000); mouse anti –beta-tubulin III antibody (clone Tuj1, Biolegend, 1:1000); rabbit anti-cleaved caspase 3 (Cell Signaling, 1:300); rabbit anti-TrkB (Abcam 1:500); rabbit anti-TrkC (Cell Signaling 1:500). The secondary antibodies were all AlexaFluor labeled (Thermo Fischer Scientific) diluted 1:500. The nuclei were labeled with Hoechst (33342, Thermo Fischer Scientific, 1:10000). Samples were mounted in VECTASHIELD Antifade Mounting Medium (H-100-10, Vector laboratories). Cell culture images were acquired with a Leica DMLB equipped with a DC300 F camera (Leica Microsystems CMS, Mannheim, Germany). Tissue was imaged with a Leica SP8 Confocal Laser Microscope (Leica Microsystems CMS, Mannheim, Germany).

Proteomic analysis

Sample preparation. Samples were prepared in randomized order and handled all together (n = 25 male mice were used in this experiment, including WT mice treated with placebo (n = 7), 5xFAD mice treated with placebo (n = 8), and 5xFAD mice treated with BNN27 (n = 10)) to avoid batch effects. Individual hippocampi were homogenized in 1 mL 5 mM HEPES/NaOH pH 7.4, 0.32 M Sucrose and Protease Inhibitor cocktail (Roche), using a tissue homogenizer in 900 rpm, 12 strokes (Schuett biotec.de homgenplus). The extract was centrifuged at 1000 x g for 10 min, 4 °C. Supernatants were transferred to new tubes, and centrifuged at 25000 x g for 40 min, 4 °C. The pellet, P2 fraction, was resuspended in Hepes buffer. Protein concentration was determined by Bradford assay (Bio-rad, Eppendorf BioPhotometer). 25 µg of each sample were mixed with SDS loading buffer, boiled at 98 °C for six min, and ran in the SurePAGE Bis-Tris gels (GenScript) for approximately 10 min at 120 V. The gels were fixed in 50% (v/v) ethanol and 3% (v/v) phosphoric acid and stained with Colloidal Coomassie Blue ((34% (v/v) methanol, 3% (v/v) phosphoric acid, 15% (w/v) ammonium Sulfate, and 0.1% (w/v) Coomassie brilliant blue G-250 (Thermo Scientific)) for 30 sec, while shaking. The gels were washed in water.

The in gel-digestion protocol was performed as previously described [73, 74]. In brief, each gel lane was sliced and cut into blocks of approximately 1 mm^3 and collected in a 96-well filter plate (MultiScreenHTS HV Filter Plate, 0.45 µm, clear, non-sterile, Millipore; Eppendorf White Deepwell plate 96/500, Eppendorf). Gel fragments were destained in 50 mM NH_4HCO_3 and 50% (v/v) acetonitrile, dehydrated using 100% acetonitrile, and rehydrated in 50 mM NH_4HCO_3 containing 10 µg/mL trypsin (sequence grade; Promega). After incubation overnight at 37 °C, peptides were extracted twice from the gel pieces with a solution containing 0.1% (v/v) trifluoroacetic acid and 50% (v/v) acetonitrile for 30 min. The solutions were collected in new tubes, dried using a SpeedVac (Eppendorf), and stored at − 20 °C until LC-MS analysis.

Peptides were dissolved in 0.1% acetic acid and were analyzed by micro LC MS/MS using an Ultimate 3000 LC system (Dionex, Thermo Scientific) coupled to the TripleTOF 5600 mass spectrometer (Sciex). Peptides were trapped on a 5 mm Pepmap 100 C18 column (300 µm i.d., 5 µm particle size, Dionex) and fractionated on a 200 mm Alltima C18 column (300 µm i.d., 3 µm particle size). The concentration of acetonitrile in 0.1 M formic acid was increased from 5 to 18% at 88 min, to 25% at 98 min, to 40% at 108 min and to 90% at 110 min. The flow rate was 5 µL/min. Peptides were electro-sprayed into the TripleTOF 5600 mass spectrometer (Sciex), with a micro-spray needle voltage of 5500 V and analyzed by data independent acquisition (SWATH). Each SWATH cycle consisted of a parent ion scan of 150 msec followed by 8 Da SWATH windows, with scan time of 80 msec, through 450–770 m/z mass range. The collision energy for each window was calculated for a 2+ ion appropriate collision energy, centered upon the window with 15 eV spread, as was previously described [75].

Data analysis and statistical analysis for proteomics. Proteomics data analysis of the raw files was performed using Spectronaut 14 software (Biognosys). An internal spectral library was created by directDIA analysis on all the samples against the mouse databases (UP000000589_10090.fasta and UP000000589_10090_additional. fasta). The Mass Spectrometry Downstream Analysis Pipeline (MS-DAP) (version beta 0.2.5.1) (https://github.com/ftwkoopmans/msdap) [76] was used for quality control and candidate discovery. Differential abundance analysis between groups was performed on log transformed protein abundances. Empirical Bayes moderated t-statistics with multiple testing correction by False Discovery Rate (FDR), as implemented by the eBayes functions from the limma R package, was used as was previously described [75]. Gene Ontology, Molecular Function and Biological process enrichment tests were performed using g:Profiler. The mass spectrometry proteomics data were deposited to the ProteomeXchange Consortium via the PRIDE [77] partner repository with the dataset identifier PXD044699.

Cell counts and quantification

For in vitro experiments, the number of BrdU (+) or TUNEL (+) or Cleaved Caspase-3 (+) cells in each culture was counted using an objective (× 32) under an inverted fluorescent microscope (Leica DMLB equipped with a DC300 F camera, Leica Microsystems CMS, Mannheim, Germany) from 4-6 visual fields for every condition. The number of BrdU (+) or TUNEL (+) or Cleaved Caspase-3 (+) cells was then counted using the unbiased cell counter offered by ImageJ (Fiji). The average number of BrdU (+) or TUNEL (+) or Cleaved Caspase-3 (+) cells to the total cell number of Hoechst (+) -stained cells was estimated for each individual photo. Finally, the percentage of BrdU (+)/Nestin (+) or TUNEL (+)/ Tuj1 (+) or Cleaved Caspase-3 (+)/Tuj1 (+) cells was normalized to the control condition. Mean was estimated for each condition from three independent experiments. Percentage of total area was calculated by ImageJ analysis.

For in vivo co-localization experiments, confocal analysis under ×40 oil lenses was conducted. The percentage of double-labeled cells for each marker was estimated by counting the cells in the DG of 6 photos of 4 mice of each subgroup. Based on a modified unbiased stereology protocol, one out of every six adjacent sections were chosen and processed for BrdU and DCX immunohistochemistry. To measure the total volume of DG, the area of granular cell layer was outlined and computed using images in every 6th adjacent section for a total of 10 sections in photos taken by a confocal fluorescence microscope (Leica SP2 confocal microscope).

Data analysis

For behavioral experiments, data were analyzed using two-way analysis of variance (ANOVA) followed by Bonferronis's *post hoc* test when appropriate. The difference in Aβ plaque load between study groups was determined by employing Student's *t*-test. For further immunohistochemistry, immunocytochemistry and biochemical data, statistical significance was assessed by paired t-test, one or two- way ANOVA analysis of variance followed by Sidak's or Bonferroni's multiple comparisons test. Statistical analysis was performed using GraphPad Prism 8.0 (GraphPad Software Inc., LaJolla, CA, USA). Sample size required in each case was estimated based on the number of groups and the expected effect size with G*power statistics software (Düsseldorf, Germany). For all comparisons, $P < 0.05$ was considered as statistical significance level.

RESULTS

BNN27 attenuates AD-related pathologies in the hippocampus of the 5xFAD mouse model

We firstly investigated whether the 60-day administration of BNN27 was capable of reducing the Aβ load in the hippocampus of the 5xFAD mice which is the region mainly responsible for spatial working memory. Immunostaining analysis using the Aβ-specific antibody 6E10 showed a significant decrease in the number of Aβ-immunoreactive plaques load in the hippocampus of BNN27 treated mice 5xFAD mice compared to placebo (Fig. 1A, B). Specifically, there were 23.78 ± 2.702 Aβ-immunoreactive plaques in the hippocampal area of the placebo treated 5xFAD mice that were significantly reduced down to 13 ± 1.764 plaques ($P_{Student's\ t\ test} = 0.0042$, t = 3.340, df = 16) in the hippocampi of the BNN27 treated animals (Fig. 1C). Noticeably, BNN27 did not restored the genotype-observed reduction in neurofilament levels on the entorhinal cortex (Supplementary Fig. S1, A, B), indicating that the duration of BNN27 administration and/or the age of the mice were not sufficient for maintaining neuronal survival on the neuronal plexus which innervate the hippocampus. The first projection of the hippocampus occurs between the entorhinal cortex (EC) and the dentate gyrus (DG). At the same time the entorhinal area is the first region, where the plaques and tangles are deposited in AD patients [78]. The EC was chosen as a region of interest due to its well described hippocampal innervation. We also examined the myelin condition in the same brain region, where there was no effect of the genotype or the treatment (Supplementary Fig. S1C, D).

Neuroinflammation is a hallmark of AD brain and is characterized by the presence of activated astrocytes and microglia [for review see: [13, 79] and similarly to other APP transgenic models [80, 81] the 5xFAD mice have elevated inflammation markers and gliosis associated with Aβ deposits commencing around two months of age [62]. We thus explored the effect of BNN27 on astrogliosis and microgliosis. Immunostaining analysis for glial activation markers GFAP (astrocytes) and IBA1 (microglia) (Fig. 1D) confirmed that by 3.5 months of age the 5xFAD mice have significantly increased astrocytic and microglial activation in the hippocampus (effect of genotype GFAP: $P_{Two\text{-}way\ ANOVA} < 0.0001$, $F_{(1,\ 27)} = 129.6$; effect of genotype IBA1: $P_{Two\text{-}way\ ANOVA} < 0.0001$, $F_{(1,\ 27)} = 65.96$). Specifically, in the 5xFAD animals there is increased activation of the astrocytes measured by the percentage area of the hippocampus covered by GFAP positive signal (4.905 ± 0.2101 vs 14.43 ± 0.7730, $P_{Bonferroni\ posttests} < 0.0001$) and increased microgliosis measured by the percentage area of the hippocampus depicted by IBA1 positive signal (4.494 ± 0.3398 vs 11.75 ± 0.4982, $P_{Bonferroni\ posttests} < 0.0001$) in comparison with the WT animals (Fig. 1E, F). Interestingly, BNN27 treatment had a significant reducing effect on the extent of astrocytic and microglial activation in the hippocampus of the animals (overall effect of the treatment GFAP, $P_{Two\text{-}way\ ANOVA} < 0.0001$, $F_{(1,\ 27)} = 58.29$; overall effect of the treatment IBA1, $P_{Two\text{-}way\ ANOVA} < 0.0001$, $F_{(1,\ 27)} = 34.50$). Next, we compared the BNN27 treated and untreated (placebo) 5xFAD mice, showing that BNN27 significantly reduced both astrogliosis and microgliosis back to control (wt) levels. Specifically, in the BNN27 treated 5xFAD mice the percentage area of the hippocampus covered by GFAP positive signal (6.8585 ± 0.4484 vs 14.43 ± 0.7730, $P_{Bonferroni\ posttests} < 0.0001$) and the percentage area of the hippocampus depicted by IBA1 positive signal (5.512 ± 0.465 vs 11.75 ± 0.4982, $P_{Bonferroni\ posttests} < 0.0001$) are reduced when compared to placebo 5xFAD mice (Fig. 1E, F). It should be mentioned here that our initial protocol for the in vivo testing of BNN27 in the 5xFAD mice was by administrating the compound for two months also but starting at 4 months old mice and isolating their brains at the age of 6 months. However, neither Aβ reduction or decrease of

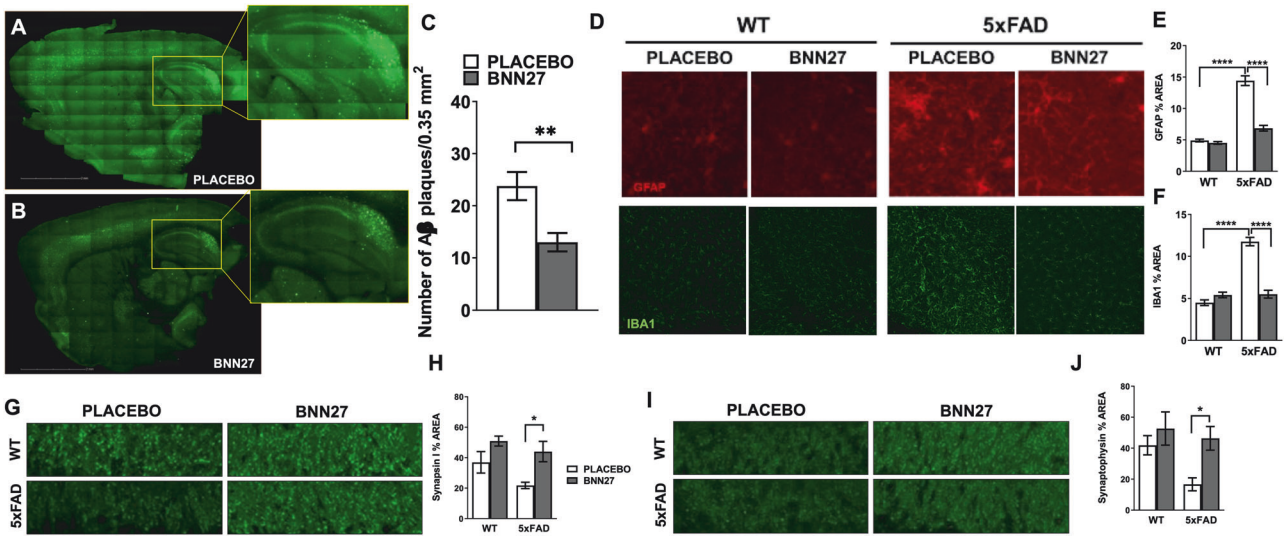

Fig. 1 Histopathological assessment of the BNN27 treated animals. Evaluation of the Aβ plaque load within the hippocampus of the 5xFAD animals [**A**, **B**] showed that the BNN27 treatment significantly decreased ($P_{Student;s\ t\ test} = 0.0042$) the formation of Aβ plaques in the area of the hippocampus [**C**] (n = 9). Immunostaining for astrogliosis (GFAP, top-panel) and microgliosis (IBA1, bottom panel) in the hippocampus of placebo and BNN27 treated animals [**D**]. There was an overall effect of the treatment [$P_{Two\text{-}way\ ANOVA} < 0.0001$] and genotype [$P_{Two\text{-}way\ ANOVA} < 0.0001$] in the astrogliosis and microgliosis. In the 5xFAD animal there is increased activation of the astrocytes [$P_{Bonferroni\ posttests} < 0.0001$] and the microglia [$P_{Bonferroni\ posttests} < 0.0001$] compare to the WT animals [**E**, **F**]. Moreover, in the 5xFAD animals BNN27 treatment significantly reduced astrogliosis [$P_{Bonferroni\ posttests} < 0.0001$] and microgliosis in the hippocampus [$P_{Bonferroni\ posttests} < 0.0001$] (n = 7–9). Immunostaining for Synapsin I in the CA2 mossy fibers of the hippocampus of placebo and BNN27 treated animals [**G**]. There was an overall effect of the treatment ($P_{Two\text{-}way\ ANOVA} = 0.0138$) in SYNAPSIN I. Moreover, in the 5xFAD animals BNN27 treatment significantly ($P_{Bonferroni\ posttests} < 0.05$) increased SYNAPSIN I staining in the mossy fibers of the hippocampus (n = 6–9) [**H**]. Immunostaining for Synaptophysin in the CA2 mossy fibers of the hippocampus of placebo and BNN27 treated animals [**I**] There was an overall effect of the treatment ($P_{Two\text{-}way\ ANOVA} = 0.0139$) and genotype ($P_{Two\text{-}way\ ANOVA} = 0.049$) in SYNAPTOPHYSIN staining. Moreover, in the 5xFAD animals BNN27 treatment significantly ($P_{Bonferroni\ posttests} < 0.05$) increased SYNAPTOPHYSIN staining in the mossy fibers of the hippocampus [**J**]. Graphs showing mean ± SEM; n = 6–9 *$P < 0.05$, **$P < 0.01$, ***$P < 0.0001$, ****$P < 0.0001$.

neuroinflammatory markers was observed, and thus we proceeded with the earlier administration, resembling to a prevention model.

Reactive astrocytes have been directly associated, both in vivo and in vitro, to neuroinflammation in such a way that reactive astrogliosis is considered a clear sign of neuroinflammation in the neurodegenerating brain. Just like microglia, astrocytes have two distinct activated states: the pro-inflammatory A1 reactive state and the anti-inflammatory A2 reactive state. In AD patients, the ratio between those two reactive states, especially surrounding senile plaques, is highly in favor of the neurotoxic A1 state. This observation is in accordance with the well characterized chronic inflammation in the brains of AD patients. To further evaluate the effect of BNN27 in microglia-astrocyte activity, we performed in vitro studies using isolated mouse microglia and astrocytes. As depicted in Supplementary Fig. S2, microglia cultures were treated with Aβ42 (10 μM) for 24h and their conditioned medium (MCM) was then transferred to naïve astrocytic cultures for another 24h before mRNA was collected. To determine the possible effects of BNN27, the compound (10^{-7}M) was introduced to either microglia cultures at the same time with Aβ42 or to astrocytic cultures at the same time with MCM or to both cultures at the beginning of each treatment. Although, Aβ42 cannot directly activate astrocytes, we hypothesized that induced astrogliosis could be microglia mediated. For this reason, we performed an experiment where we use Aβ42 to activate microglia and after 24h we collect the conditioned medium and transfer it to naive astrocytic cultures. After 24h of treatment with this microglia-conditioned medium (MCM), we collect RNA and repeat the RT-PCR as previously. This time, as a positive control, we performed a 24h LPS (100ng/ml) treatment on microglia cultures and then transferred the MCM to naive astrocytes. Our results (Supplementary Fig. S2) reveal successful astrogliosis as both expression levels of Steap4 and Serpina3n markers were found significantly increased, while BNN27 had no effect on this astrogliosis phenotype, suggesting that factors involved in the anti-inflammatory effects of BNN27 are missing in the in vitro cultures. After having established our protocol for Aβ42-mediated astrocytic activation, we estimated the relative amount of A1 and A2 astrocytes in these cultures. For this reason, we selected specific target genes whose overexpression has been associated with A1 population respectively. For the A1 population, we have chosen Amigo2, Srgn and Serping1 genes. Polypeptide Aβ was able to induce the expression of these pro-inflammatory astrocytic markers while BNN27 reduced their levels, especially Srgn and Serping1. (Supplementary Fig. S2, B, C).

Oakley et al. (2006) [62] reported synaptic degeneration, assessed with whole-brain levels of the presynaptic marker synaptophysin as early as four months of age of 5xFAD mice. Given our observations that BNN27-treated animals show improved Aβ plaque pathology and reduced gliosis in the hippocampus, we hypothesized that these changes might be associated with reduced synaptic degeneration in the BNN27-treated brain. Therefore, we evaluated the synaptic button load using two different markers (Synaptophysin and Synapsin I) in the CA2 mossy fibers of the hippocampus of 5xFAD mice. Immunostaining analysis for Synaptophysin and Synapsin I (Fig. 1G, I) confirmed that four month of age 5xFAD mice show significant synaptic loss in the hippocampus (effect of genotype Synaptophysin: $P_{Two\text{-}way\ ANOVA} = 0.0490$, $F_{(1,\ 21)} = 4.365$). Interestingly, BNN27 treatment significantly rescued synaptic degeneration in the hippocampus (overall effect of the treatment Synapsin I, $P_{Two\text{-}way\ ANOVA} = 0.0054$, $F_{(1,\ 21)} = 9.605$; overall effect of the treatment Synaptophysisn, $P_{Two\text{-}way\ ANOVA} = 0.0139$, $F_{(1,\ 27)} = 7.197$). BNN27 significantly reduced the synaptic loss, measured as percentage area of the CA2 mossy fibers of the hippocampus covered by Synaptophysin (16.68 ± 4.194 vs 46.34 ± 7.641, $P_{Bonferroni\ \ posttests} = 0.0352$) or Synapsin I positive signal (21.79 ± 2.109 vs 44.01 ± 6.704, $P_{Bonferroni\ \ posttests} = 0.0433$) when compared to the placebo 5xFAD mice (Fig. 1H, J).

BNN27 rescues the cholinergic atrophy at the basal forebrain of the 5xFAD animals

Cholinergic neurons, especially those in the basal forebrain, are known to be particularly susceptible in AD [5–7]. In the 5xFAD mice, in particular, the lesion of cholinergic fibers occurs earlier than the cholinergic neuron loss with the basal forebrain being the first brain region where cholinergic neuron loss is observed at the age of 9 months [82].

First, we aimed to evaluate the integrity of the cholinergic neurons at the basal forebrain of the 5xFAD mice using the choline acetyltransferase (ChAT) expression as a marker for identifying cholinergic neurons (Fig. 2A). Indeed, ChAT+ neurons in the BF of the 5xFAD mice have significantly smaller soma size when compared with the WT animals (67.9832 ± 5.722 vs 52.00 ± 2.8008, $P_{Bonferroni\ posttests} = 0.0485$) (Fig. 2B). The administration of BNN27 effectively restored the size of cholinergic neurons, indicating a protective role and potentially recovery of their functionality.

We have previously shown that the neuroprotective and neurogenic effects of BNN27 are mediated by the TrkA and p75NTR receptors [56, 57]. Thus, we hypothesized that the expression of these receptors may be altered in the ChAT+ neurons of the BF. Interestingly, no change was observed in the expression of TrkA receptor in the ChAT+ neurons since the number of the double positibe TrkA+/ChAT+ neurons remained unaltered (Fig. 2C). However, the number of p75NTR+/ChAT+ neurons at the BF of the 5xFAD animals was significantly increased compared to the WT ($P_{Bonferroni\ posttests} = 0.0317$). Moreover, in the 5xFAD animals, BNN27 treatment significantly reduced the number p75NTR +/ChAT+ neurons ($P_{Bonferroni\ posttests} = 0.0198$) in the basal forebrain compared to 5xFAD placebo animals (Fig. 2D, E), indicating the p75NTR significance in disease progress.

Neuroprotective effect of BNN27 in hippocampal neuronal cultures against oligomeric Aβ-induced toxicity

Based on the neuroprotective effects of BNN27 in vivo in the hippocampal region of 5xFAD mice, we sought to investigate its effects on the neurotoxicity of Aβ, in isolated E17.5 mouse hippocampal neurons, expressing TrkA and p75NTR receptors (Supplementary Fig. S3). Due to well documented pro-survival effect of neurotrophins through Trk receptors, we investigated whether BNN27-induced activation of TrkA and/or p75NTR receptors is also neuroprotective against Aβ. The oligomeric neurotoxic Aβ42 allomorph was introduced in the culture, since predominate in the deposits of 5 μM Aβ42 in the human brain [83–85]. We used the In Situ Cell Death Detection Kit (TUNEL, Sigma-Aldrich) to measure cell death. The TUNEL reaction indicates DNA strand breaks that occur during apoptosis, distinguishing apoptosis from necrosis. To localize hippocampal neurons in the initial stage of neuronal differentiation we utilized the widely-used neuronal marker of the central and peripheral nervous system, Tuj1 (class III beta-tubulin).

The addition of Aβ for 48 h in the culture managed to increase the levels of TUNEL (+) 8DIV neuronal cells compared to the healthy complete nutrient medium (CTR) condition by a percentage of ≃40% (*P <0.01, Fig. 3A–C). More importantly, BNN27 showed a strong neuroprotective effect significantly reducing the Aβ-induced increase in the percentage of TUNEL (+) cells (*P <0.01).

To determine the potential effect of Aβ on more 'mature' neuronal cultures, illustrating the differences occurring throughout the development in in vitro neuronal cultures, hippocampal neurons were utilized in a later developmental stage of 12DIV. The development of hippocampal neurons in culture has been the subject of a remarkable number of studies. Thus, we know that

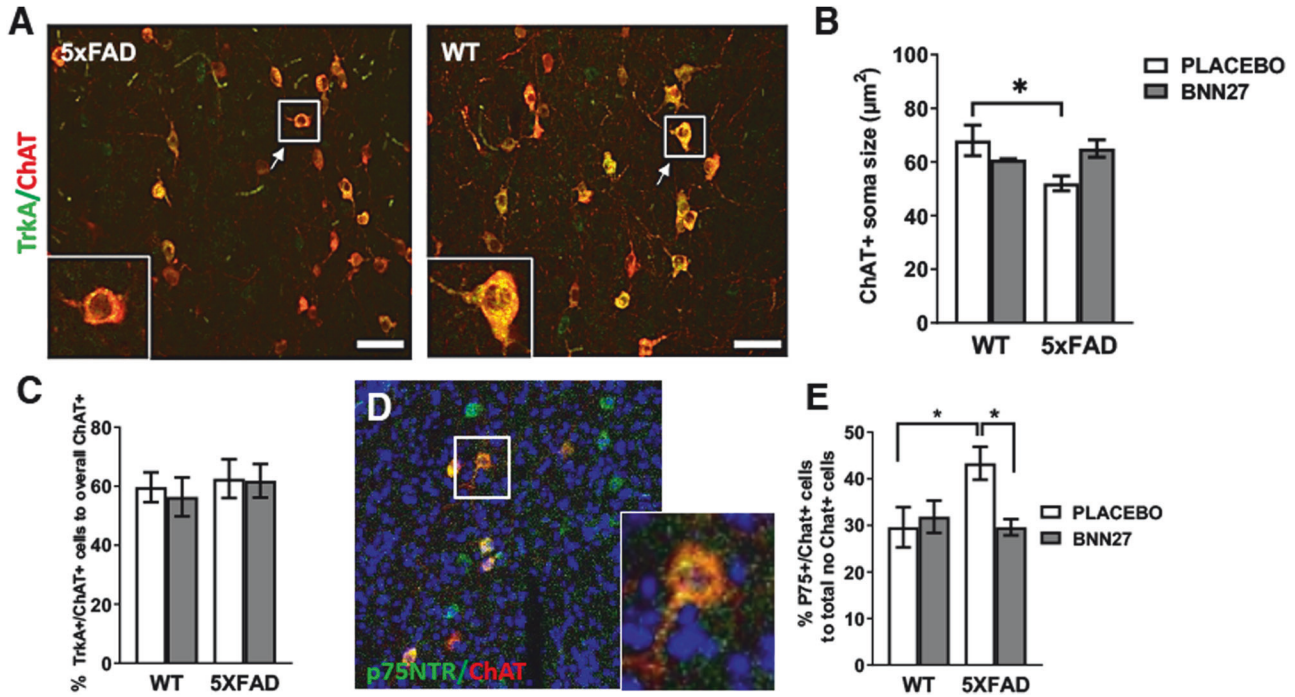

Fig. 2 Reduced cholinergic atrophy in the basal forebrain of the BNN27 treated mice. Representative image of TrkA immunostained cholinergic neurons (ChAT+) in the basal forebrain (BF) [**A**]. In the 5xFAD placebo mice there was a significant reduction in ChAT positive neurons soma size ($P_{Bonferroni\ posttests} = 0.0485$) when compared with the WT placebo animals [**B**]. No change was observed in the percentage of double positive TrkA+/Chat+ neurons between genotypes or treatments [**C**]. Representative images of p75NTR immunostained cholinergic neurons (ChAT+) in the basal forebrain [**D**]. There was a significant increase in the percentage p75NTR +/ChAT+ neurons at the BF of the 5xFAD animals compared to the WT ($P_{Bonferroni\ posttests} = 0.0317$). Moreover, in the 5xFAD animals, BNN27 treatment significantly reduced the percentage p75NTR +/ChAT+ neurons ($P_{Bonferroni\ posttests} = 0.0198$) in the basal forebrain compared to 5xFAD placebo animals [**E**]. Graphs showing mean ± SEM; n = 4 *P < 0.05, **P < 0.01, ***P < 0.0001, ****P < 0.0001.

12DIV are regarded an adequate time interval to initiate the treatment, since nerve cell bodies have expanded in size, a complex and intertwined axonal network and sufficient dendrite network [86]. Cleaved Caspase-3 is considered a key factor of apoptotic proteolysis, serving as a marker of programmed cell death. Recent evidence implicates that this protease in involved in the pathogenesis of neurodegenerative diseases [87]. The introduction of Aβ42 in the culture of 12DIV hippocampal neurons increased the percentage of cleaved Caspase-3(+) / Tuj1(+) cells almost twice compared to the complete nutrient medium (CTR), an increase that was significantly reduced in the presence of BNN27 (*P<0.05) (Fig. 3D, G).

The p75NTR inhibitor was able to significantly decrease the levels of cleaved Caspase-3(+) / Tuj1(+) neurons (**P<0.01, Fig. 3F, G). It is of particular note, that the reducing effect of BNN27 on caspase-3 activation was obliterated by the presence of p75NTR inhibitor in the E17.5 hippocampal neuronal culture, suggesting that the p75NTR receptor was mediating its action [Fig. 3D–F]. The involvement of p75NTR receptor in the above effect of BNN27, was further supported by the stimulatory effects of Aβ, NGF or BNN27 on the p75NTR post-receptor TRAF6 signaling pathway (Supplementary Fig. S4).

To simulate the long-term effects of Aβ in the brain of patients with AD, we cultured 12DIV hippocampal cells with 5 μM Aβ42, for 6 days, adding every 2 days in the culture media the NGF, the proNGF, or BNN27. In 'mature' 12DIV cultured neurons, only less than 30% displayed apoptosis in basal conditions (Fig. 3K–M). In contrast, Aβ42 increased the percent of apoptotic cells nearly three-fold (***P<0.001). Interestingly, in agreement with our previous observations, BNN27 was able to alleviate the 'chronic' Aβ pathology in 6 days 12DIV hippocampal cell cultures (**P<0.01). These findings suggest that BNN27 can effectively control long-term Aβ neurotoxicity.

BNN27 promotes adult neurogenesis in the hippocampus of the 5xFAD mice

The dentate gyrus (DG) is a critical component of the hippocampal circuit involved in episodic and spatial memory [88]. The subgranular zone (SGZ) of the DG is one of the two areas that undergo neurogenesis in the adult brain [89, 90]. Given the well described neurotrophin actions of the BNN27 and its neuroprotective effects in the 5xFAD animals, we investigated whether BNN27 exerts also neurogenic effect in the SGZ of the DG. Initially, we evaluated the incorporation of BrdU in neurons (NeuN positive cells) located at the SGZ by measuring the number of BrdU+/NeuN double positive cells in the DG of the animals (Fig. 4A, B). Interestingly, there was an overall effect of the treatment ($P_{Two\text{-}way\ ANOVA} = 0.0007$, $F_{(1,\ 13)} = 19.68$) suggesting that BNN27 significantly increases the number of BrdU+/ NeuN double positive cells. In addition, there was an overall effect of the genotype ($P_{Two\text{-}way\ ANOVA} = 0.0011$, $F_{(1,\ 13)} = 17.44$) in the number of BrdU+/NeuN+ neurons suggesting that the 5xFAD mice have reduced neurogenic potential at the age of 4 months old. BNN27 treatment in the 5xFAD mice significantly increases the number of BrdU positive neurons in the DG of the hippocampus compared to 5xFAD placebo animals (456 ± 56.349 vs 858 ± 4.472. $P_{Bonferroni\ posttests} = 0.0032$) (Fig. 4C).

The neurogenic effect of BNN27 was also evaluated by measuring the number of Doublecortin (DCX) positive neurons in the DG of the 5xFAD mouse hippocampus (Fig. 4D). DCX is a microtubule-associated protein expressed by neuronal precursor cells and immature neurons and a marker of newly born neurons. There was an overall effect of the treatment ($P_{Two\text{-}way\ ANOVA} = 0.0097$, $F_{(1,\ 13)} = 9.179$) and genotype ($P_{Two\text{-}way\ ANOVA} = 0.0007$, $F_{(1,\ 13)} = 19.32$) in the number of DCX+ neurons suggesting that BNN27 significantly increases the number DCX+ neurons in the 5xFAD animals which have impaired incorporation of DCX+

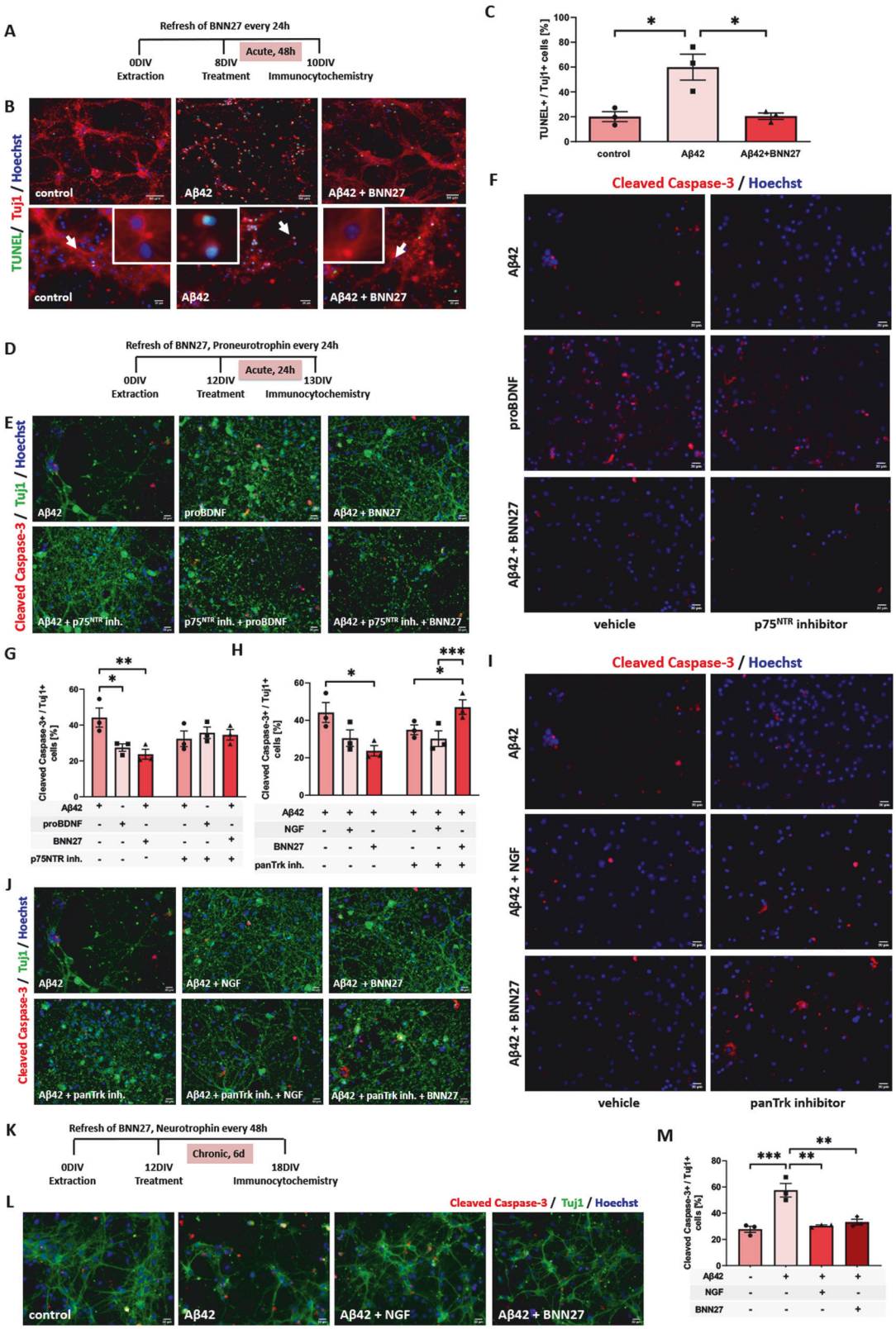

neurons in their DG under basal conditions. However, in the 5xFAD animals, BNN27 treatment significantly increases the number of newly born neurons in the DG of the hippocampus compared to the 5xFAD placebo animals (82.2 ± 5.38 vs 106.8 ± 5.737, $P_{Bonferroni\ posttests} = 0.011$) (Fig. 4E).

BNN27 protects the hippocampal Neural Stem Cells against oligomeric Aβ-induced toxicity

To further explore the neurogenic properties of BNN27, we used isolated adult (P7) Neural Stem Cells (NSCs) treated with the Aβ peptide (a 5 μM concentration of oligomeric Aβ42 peptide was

Fig. 3 BNN27 reverses the Aβ40 induced toxicity in the E17.5 immature hippocampal neurons. A Illustrative graph that shows the 'acute' 48h administration of BNN27 and proneurotrophin in the E17.5 mature hippocampal neuronal culture and the initiation of the immunocytochemistry (ICC) experiment. **B** Representative images of immunofluorescence with TUNEL (green), Tuj1 (red), Hoechst (blue) conditions in the presence of Aβ vs the complete medium (CTR) condition. **C** Quantification of TUNEL (+) / Tuj1 (+) cells under 48 h of Aβ40 (5 μM) administration to E17.5 hippocampal neurons in the presence and absence of BNN27 (1-way ANOVA, Bonferroni multiple comparison test). p75NTR - not Trk receptors - seem to be implicated in the established effect. **D** Illustrative graph that shows the 'acute' 24h administration of BNN27 and proneurotrophin in the E17.5 mature hippocampal neuronal culture and the initiation of the immunocytochemistry (ICC) experiment. **E** Immunofluorescence with Cleaved Caspase-3 (green), Hoechst (blue) and [**F**] Tuj1 (green) conditions in the presence or absence of Aβ [Aβ40, 5 μM)] and/or p75NTR inhibitor [anti-p75 Receptor antibody (MC-192) Abcam], proBDNF and BNN27. **G** Quantification of TUNEL (+) / Tuj1 (+) cells under a 24 h administration of Aβ, p75NTR inhibitor treated as indicated at a 12DIV hippocampal neuronal cell culture (1-way ANOVA, Bonferroni multiple comparison test). **H** Quantification of TUNEL (+) / Tuj1 (+) cells under a 24 h administration of Aβ, panTrk inhibitor (AZD-1332, Alomone) treated as indicated at a 12DIV hippocampal neuronal cell culture (1-way ANOVA, Sidak's multiple comparison test). **I,J** Immunofluorescence with Cleaved Caspase-3 (green), Hoechst (blue) and Tuj1 (green) conditions in the presence or absence of Aβ [Aβ40, 5 μM)] and/or panTrk inhibitor, NGF and BNN27. BNN27 affects the reciprocal extensive exposure to the Aβ40 toxicity at the E17.5 mature hippocampal neurons **K** Illustrative graph that shows the exact time periods for drug administrations and the immunocytochemistry (ICC) induction [**L**] Representative images of Cleaved Caspase-3 (red), Tuj1 (green), Hoechst (blue) staining of hippocampal 12DIV neurons after Aβ induction in the presence or absence of NGF, BNN27. The complete medium (CTR) condition serves as positive control. The images were taken at ×32 magnification (Scale bar, 20 μM). **M** Quantification of Cleaved Caspase-3 (+) / Tuj1 (+) after chronic administration (6 days) of NGF, BNN27 in order to test their 'long term' effects in the primary neuronal cell culture, with simultaneous injection of Aβ40 (5 μM) (1-way ANOVA followed by Sidak's multiple comparison test) Data are expressed as mean ± SEM; $^{*}P < 0.05$, $^{**}P < 0.01$, $^{***}P < 0.001$, n = 3; Scale bar = 20 μm.

utilized), in order to define compound's effect on neural stem cell fate. The allomorph with the longest length Aβ42 tends to form higher molecular weight oligomers than the other isoforms, followed by conversion to protofibrils and mature fibrils, indicating that the accumulation of Aβ42 could predominate in the early stages of the Alzheimer's Disease [83–85]. The toxicity of the Aβ was evaluated in a bilateral manner.

The effects of BNN27 on neural stem cell proliferation was firstly evaluated. Survival of the progeny of the dividing progenitor cells was assessed by staining for 5-Bromo-2'-deoxyuridine (BrdU) incorporation. NSCs progeny from the hippocampus were plated on poly-L-lysine and Laminin. Nestin is a well-established marker of neuronal progenitor cells in the adult brain [91]. A significant decrease by almost 30% of BrdU(+)/Nestin (+) cells was found in NSC cultures in the presence Aβ42 compared to cells in the Complete medium. However, neither the injected NGF nor BNN27 were able to restore the decreased BrdU (+)/Nestin (+) cell ratio (Fig. 5A, B).

In order to evaluate the cell protective effects of BNN27 in NSCs, hippocampal P7 neurospheres were treated with the BNN27, the Brain-Derived Neurotrophic Factor (BDNF) or the pro-BDNF in the presence of Aβ42. A 48-h exposure of NSCs in oligomeric Aβ42 allele is sufficient to increase the levels of cytotoxicity in the culture (*** P<0.0001, Fig. 5C, D), as detected by the CellTox Green Cytotoxicity Assay (Real-time Cell Death Assay, Promega). BNN27 was effective to protect against Aβ toxicity (**P<0.05), as well as BDNF (** P<0.05) (Fig. 5C, D).

To evaluate further the implication of the neurotrophin receptors in the aforementioned result, the experimental procedure was recapitulated only this time in the presence of panTrk (AZD-1332, Alomone) and p75NTR [anti-p75 Receptor antibody (MC-192), Abcam] inhibitors. Interestingly, the established in vitro neuroprotective effect of BNN27 compound was abolished in the presence of whether panTrk or p75NTR inhibitor (* P<0.01). In particular, BNN27-induced activation of Trk receptors and p75NTR receptors – both – were shown to significantly reduce in vitro the Aβ oligomer-injected cytotoxicity (Fig. 5E–H).

In order to explore a potential direct neurotrophic effect of BNN27 in adult (P7) NSCs, we exposed cultures of NSCs to BNN27 and a low concentration of neurotrophic EGF in the absence of FGF, for 24 and 48 h. BNN27 significantly increased the proliferation of P7 hippocampal NSCs within 24h, even in reduced levels of EGF (5 ng/ml, absence of FGF) (Supplementary Fig. S4, C, D), suggesting that BNN27 might serve as a sufficient trophic factor under conditions where the endogenous trophic support is limited. However, at 48 h, BNN27 was able to induce the proliferation of P7 hippocampal NSC only with reduced concentration of EGF and not under a complete deprivation of growth factors (Supplementary Fig. S5, A–F).

Furthermore, we tested the neurogenic effects of BNN27 on the other neuronal population of proliferating cells, the Oligodendrocyte Precursor Cells (OPCs). Upon isolation of OPCs from P3 pups, we cultured them in proliferation medium (containing PDGF, FGF) for two days, then cultures were exposed to 1 μM BNN27 for 48hrs. Subsequently, a 24hr BrdU pulse was performed. Co-staining for PDGFR and BrdU showed that BNN27 significantly promoted OPC proliferation, increasing the number of PDGFR +/BrdU+ cells by ~20% (Supplementary Fig. S6a), establishing BNN27 as a strong neurogenic agent. Furthermore, we also examined the BNN27 effect on oligodendrogenesis by evaluating OPCs maturation. OPCs were cultured for another 48hrs in differentiation medium (containing T3) in the presence of amyloid beta 1-42 (5 μM). Immunofluorescence analysis showed that BNN27 was capable of increasing O4+ cells as well as NGF did under neurodegenerative conditions (Supplementary Fig. S6b).

BNN27 reduces spatial memory deficits in the 5xFAD mice

It is well documented that the 5xFAD mice by 4–5 months of age have significantly impaired spontaneous alternation performance which translates into spatial working memory deficits [62]. Based on the aforementioned cellular effects of BNN27 in the 5xFAD brain, we investigated whether BNN27 has a protective effect in hippocampal-dependent spatial working memory too. We assessed spontaneous alternation performance in the T-maze in mice, receiving for 2 months either BNN27 or placebo (introduced as subdermal pellets steadily releasing 10mg/kg/day, Fig. 6A). The T-maze used was an elevated apparatus in the form of a T placed horizontally (Fig. 6B) (see "Methods" part for protocol's details). This learning task does not involve any training, reward, or punishment and allowed us to assess hippocampus-dependent spatial working memory.

BNN27 and placebo-treated for 60 days 5xFAD mice as well as age-matched wild type control mice had their spontaneous alternation performance evaluated. Two-way ANOVA analysis, with the genotype and the treatment as the two independent variables, showed that there is an overall significant effect of the treatment ($P_{two\text{-}way\ ANOVA} = 0.0007$, $F_{(1,\ 27)} = 14.71$) and genotype ($P_{two\text{-}way\ ANOVA} = 0.0408$, $F_{(1,\ 27)} = 4.616$) in the spontaneous alternation performance of the mice, suggesting that 5xFAD mice perform significantly poorer than the wild type mice and that BNN27 significantly improves the performance of the 5xFAD mice. Moreover, post hoc analysis using Bonferroni's multiple comparisons test showed that in the BNN27-treated 5xFAD animals there

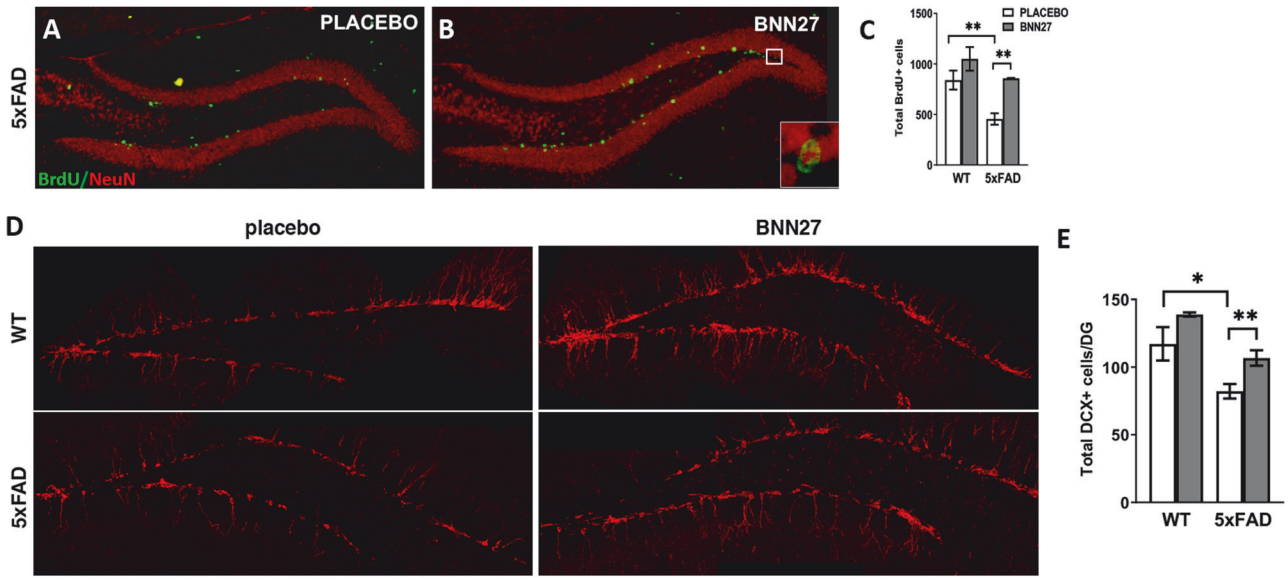

Fig. 4 BNN27 promotes adult hippocampal neurogenesis in the 5xFAD mice. Immunostaining for BrdU and NeuN in the dentate gyrus of the hippocampus of placebo and BNN27 treated 5xFAD animals [**A**, **B**]. There was an overall effect of the treatment ($P_{Two\text{-}way\ ANOVA} = 0.0007$) and genotype ($P_{Two\text{-}way\ ANOVA} = 0.0011$) in the number of BrdU+/NeuN+ neurons. Moreover, in the 5xFAD animals BNN27 treatment significantly ($P_{Bonferroni\ posttests} = 0.0032$) increases the number of BrdU positive neurons in the hippocampus compared to 5xFAD placebo animals [**C**]. Immunostaining for DCX in the dentate gyrus of the hippocampus of placebo and BNN27 treated animals [**D**]. There was an overall effect of the treatment ($P_{Two\text{-}way\ ANOVA} = 0.0097$) and genotype ($P_{Two\text{-}way\ ANOVA} = 0.0007$) in the number of DCX+ neurons [2-way ANOVA for treatment and genotype]. Moreover, in the 5xFAD animals BNN27 treatment significantly ($P_{Bonferroni\ posttests} = 0.011$) increases the number of newly born neurons hippocampus [**E**]. Graphs showing mean ± SEM; n = 4 $^{*}P < 0.05$, $^{**}P < 0.01$, $^{***}P < 0.0001$, $^{****}P < 0.0001$.

is a significant improvement in spontaneous alteration performance compared to the placebo-treated 5xFAD animals (0.643 ± 0.025 vs 0.4625 ± 0.026, $P_{Bonferroni\ posttests} = 0.0027$). This behavioral analysis fully confirmed that the neurorestorative and cell protecting effects of BNN27 are sufficient to overcome AD-derived pathology and may represent a new therapeutic approach against multifactorial neurodegenerative diseases, like AD.

BNN27 has global rescue effects on Aβ induced negative impact

We finally assessed whether there were any significant changes in the proteomes of BNN27-treated 5xFAD mice, comparing the protein expression profile of these animals to untrated 5xFAD and WT mice, using mass spectrometry analysis. We performed direct DIA analysis, considering a peptide as 'detected' if the confidence score (for identification) was ≤0.01. Proteomics analysis included 3200 proteins and 16.000 peptides per sample were identified and quantified (Supplementary Fig. S7a). The Coefficient of Variation was between 12 and 16 percent for the different groups and the peptide intensity distributions revealed high quality across all samples and low missing values, meaning that each identified peptide in a sample overlaps with other samples in the sample dataset (Supplementary Fig. S7b). The fold change of all peptides in a sample was compared to their mean value over all samples in the group. Any loading differences were corrected after normalization which visualized how strongly each sample deviates from other samples in the same group that indicated the identification and removal of one outlier sample (WT placebo), according to the mass spec run (Supplementary Fig. S7c). In order to find the significant regulated proteins, we set the q-value threshold at 0.05 and the log2 fold change threshold ≤ − 0.2 / ≥ + 0.2 and these filters were used for statistical analysis.

Aβ induces major changes that reflect the AD pathology

In the comparison between the 5xFAD and WT both treated with placebo mice group, 209 significantly dys-regulated proteins found, with 127 proteins up-regulated and 82 proteins down-regulated in the 5xFAD group. The volcano plot indicated that Aβ-induced proteins like App, Apoe, Hexb, Bace1, Ncstn were significantly up-regulated in the 5xFAD mice (Fig. 7a, Supplementary Table S1) [92–94].

In order to get a better understanding towards the changes, a g:profiler enrichment analysis was performed using the whole mouse genome as background, for both the down-regulated and the up-regulated proteins respectively (http://biit.cs.ut.ee/gprofiler/).

The enrichment analysis of down-regulated proteins showed among others, proteins implicated in the synaptic signaling as well as the glutamatergic synapse. Moreover, proteins related to neurogenesis (Lingo1, L1cam, Stxbp1) and neuron projection (Abl1, Nectin1, Gap43) were significantly down-regulated [95, 96]. Another pathway in which proteins were significantly changed was retrograde endocannabinoid signaling pathway (Gabra5, Ndufa3). Finally, molecular functions affected, were those of protein binding and calcium-dependent phospholipid binding (Syt5, Syt7, Syt17) (Fig. 7b) [97].

On the other hand, the enrichment analysis of up-regulated proteins showed changes in the complement pathway activation (e.g. C1qa, C1qb and C1qc), cholesterol biosynthesis (Nsdhl, Hmgcs1) [98], as well as, the innate immune system (Cstd, Aldoc) and neurotrophil degranulation (Cst3, Arl8a) [99]. Moreover up-regulation was observed on lysosomal (Hexb, Hexa, Lamp2), metabolic pathway (Pld3, Idi1), mitochondrion (Ank2, Ncstn), and synapse (negatively) related proteins (Bace1, Syt11). Close to that, significant up-regulation was observed in proteins indicating neuronal death (Nefl, Stat3) and proteins involved in Aβ binding and regulation of amyloid fibril formation (Apoe, App, Clu, Itm2c, Itm2b, Bace1) subsisting Alzheimer's disease. Proteins associated with pseudobulbar signs (Htra1, Sod1) and cerebral amyloid angiopathy (e.g. Iltm2b, Cst3) in the human brain, were also differentially regulated in our mouse disease-like genotype (Fig. 7c). Our proteomics data therefore validates major changes that reflecting AD pathology in the 5xFAD mice.

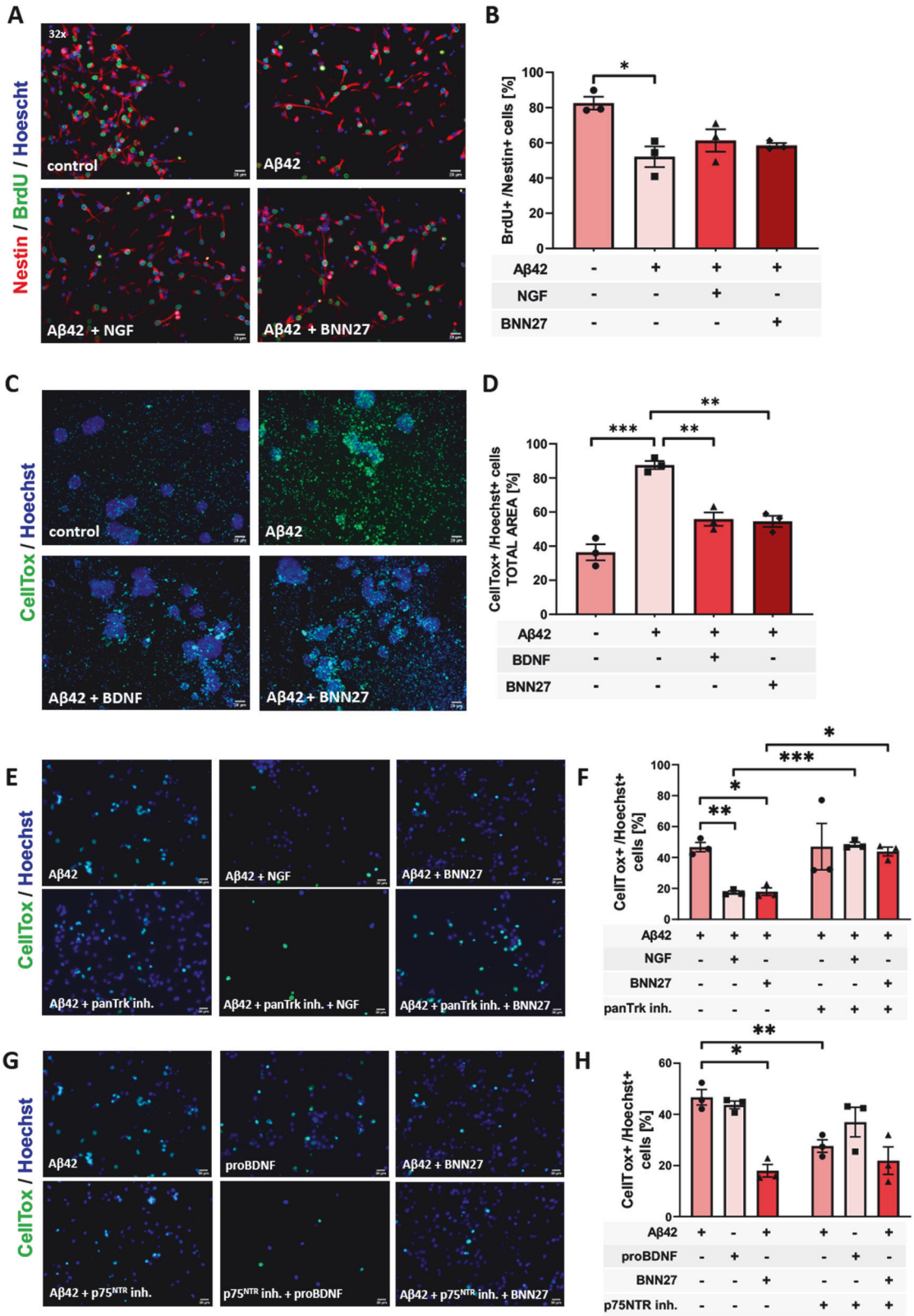

BNN27 has global rescue effects on Aβ induced negative impact in 5xFAD mice

To assess BNN27 administration effects, we compared the BNN27 treated 5xFAD mice and placebo treated WT mice. 277 proteins were significantly dys-regulated in the 5xFAD+BNN27/WT comparison from which 149 significantly regulated only in 5xFAD +BNN27/WT and 128 overlapped in both comparisons (5xFAD +BNN27/WT and 5xFAD/WT). In addition, 81 proteins were significantly dys-regulated only in the 5xFAD/WT comparison and not in the 5xFAD+BNN27/WT (Fig. 8a, Supplementary Table S2).

Fig. 5 BNN27 protects the hippocampal Neural Stem Cells from oligomeric Aβ induced toxicity. There was no detectable difference on the percentage of the BrdU(+) cells given the presence of BNN27 in the P7 Aβ-introduced NSC culture. **A** BrdU incorporation (green) evaluation of the Nestin(+) P7 NSCs (red). **B** Quantification of BrdU(+)/Nestin(+) cells under 48h induction of Aβ at the the P7 NSC hippocampal culture, in the presence or absence of NGF and BNN27 treatment, respectively. The complete condition depicts the positive control [1-way ANOVA for treatment and genotype, Sidak's multiple comparisons Post Hoc tests]. **C** Staining with CellTox Green Cytotoxicity Assay. **D** Evaluation of the in vitro cytotoxicity of Aβ42 oligomer as well as the potential 48 h neuroprotective activity of BDNF neurotrophin and BNN27 in the P7 NSCs of hippocampus. The complete medium (CTR) condition serves as positive control. [1-way ANOVA for treatment and genotype, Sidak's multiple comparisons Post Hoc tests]. Both Trk receptors and p75NTR seem to be implicated in the observed result. **E** Immunofluorescence with CellTox (green) and Hoechst (blue) conditions that shows the 24h administration in the P7 hippocampal neural stem cell culture in the presence or absence of Aβ42 (5 μM) and/or panTrk inhibitor (AZD-1332, Alomone), NGF or BNN27. **F** Quantification of CellTox (+) / Hoechst (+) cells under a 24 h administration of Aβ and/or panTrk inhibitor, treated as indicated at a P7 hippocampal neural stem cell culture (1-way ANOVA, Tukey multiple comparison test). **G** Immunofluorescence with CellTox (green) and Hoechst (blue) conditions that shows the 24h administration in the P7 hippocampal neural stem cell culture in the presence or absence of Aβ42 (5 μM) and/or p75NTR inhibitor [anti-p75 Receptor antibody (MC-192) Abcam], proBDNF or BNN27. **H** Quantification of CellTox (+) / Hoechst (+) cells under a 24 h presence or absence of Aβ and/or p75NTR inhibitor, treated as indicated at a P7 hippocampal neural stem cell culture (1-way ANOVA, Tukey multiple comparison test). Data are expressed as mean ± SEM; $*P < 0.05$, $**P < 0.01$, $***P < 0.001$, n = 3; Scale bar = 20 μm).

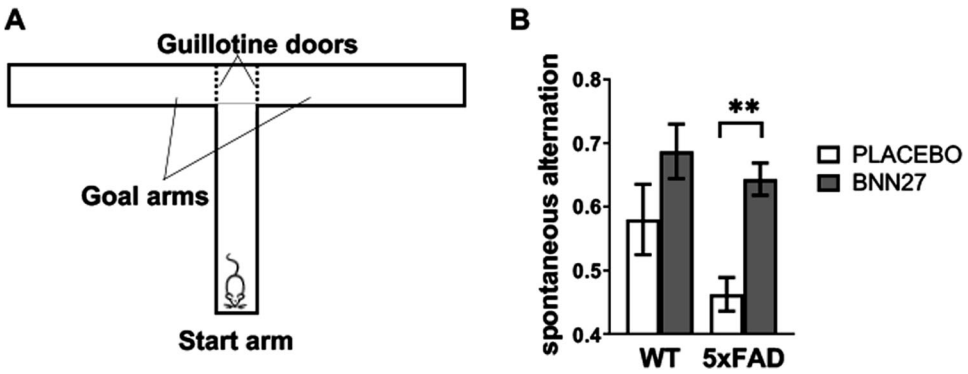

Fig. 6 Working memory evaluated in the T-maze. A Graphic representation of the T-maze apparatus. **B** Working memory was evaluate by measuring the spontaneous alternation of the mice it the apparatus. It was shown that there is an overall significant effect of the treatment [$P_{Two\text{-}way\ ANOVA} = 0.0007$] and genotype [$P_{Two\text{-}way\ ANOVA} = 0.0408$] in the spontaneous alternation performance of the mice. Moreover, in the 5xFAD animals BNN27 treatment significantly improved working memory performance ($P_{Bonferroni\ posttests} < 0.01$) [Graph showing mean ± SEM; $n = 7–9$; $**P < 0.01$).

Many of the shared proteins include the typical AD-associated proteins such as App, Clu, Apoe, Gfap, Hexb etc, which implicates that the administration of BNN27 is not capable of restoring the 5xFAD mice to the wild type level. Nevertheless, BNN27 appeared to cause a lesser up-regulation of these AD-associated proteins.

To reveal the probable partial rescue effect of BNN27, a double volcano plot was created (Fig. 8b) to reveal the "shift" in the log2 fold change of the significantly-changed proteins between the two comparisons. This "shift" between the log2 fold changes reveals a partial rescue if the log2 fold change is closer to zero after the treatment with BNN27 ((log2fc(5xFAD+BNN27/WT)) as it reveals less difference in the protein expression between the two groups (5xFAD+BNN27 and WT)" and is quantified by calculating the percentage of the change between the log2 fold changes as follows:

$$[(\log 2fc(5xFAD + BNN27/WT) - \log 2fc(5xFAD/WT))/ (\log 2fc(5xFAD/WT)] * \%$$

BNN27 treatment leads to the rescue of 16 (out of 47) down-regulated proteins by more than 10%. These proteins are implicated in the ATP-dependent protein binding (Dnajc5, Prnp) [100], the trans-synaptic signaling (Bcr, Cd38, Dagla, Gabra5, Prnp, Slc30a1), response to stress, regulation of biological quality and the synapse (Adam11, Bcr, Cd38, Dagla, Dele1, Gabra5, Gap43, Prkca, Prnp, Slc30a1, Gpc1). In addition, rescued were proteins of the somatodentritic compartment (Adama11, Bcr, Dagla, Gabra4, Gap43, Gpc1, Prnp), the cytoplasm (Nudt3, Gnb4, Gap43, Dele1), the organelle membrane (Atp85, Cd38, Dagla, Dele1, Dnajc5, Ndufs1, Prkca, Prnp, Scl30a1) [101] and the cell body (Adam11, Gabra5, Gap43, Gnb4, Gpc1) (Fig. 8c, Supplementary Table S3).

Furthermore, BNN27 treatment rescued 38 (out of 81) up-regulated proteins by leading to a decrease in the log2 fold change in the comparison 5xFAD+BNN27/WT by more than 10% compared to 5xFAD/WT mice log2 fold changes. More precisely, the rescued proteins are related to Alzheimer's disease (Apoe, Bace1, App), Aβ and amide binding (Apoe, Clu, Bace1, Itm2c, Itm2b, Clstn1), oxidative damage response and complement activation (C1qc, C1qb, C1qa), N-acetyl-beta-D-galactosaminidase and beta-N-acetylhexosaminidase activity (Hexb, Hexa), amyloid precursor protein metabolic process (Apoe, Itm2b, Clu, Bace1, Itm2c, APP), microglial and astrocytic cell activation, as well as neuro-inflammatory (C1qa, Syt11, Clu, App, Gfap), innate immune response (Actr10, Lamp2, Hexb, C1qc, C1qb, C1qa, CTsd, Ctsz), chaperone-mediated autophagy (Gfap, Lamp2, Clu) [102] and autophagy (Arl8b, Gfap, Ctsd, Atg9a, Lamp2, Syt11, Clu), synapse pruning (C1qc, C1qb, C1qa), as well as postsynaptic proteins (Sptbn1, C1qc, C1qb, C1qa, Clstn1, Syt11, App), proteins of the extracellular matrix (Spock2, Htra1, Clu, Ctsz, Ctsd) (Fig. 8d). The most rescued protein was Sptbn1 that is implicated in synapse, axon, cell projection (as well as Gfap), neuron projection and post-synapse cellular component, together with more rescued proteins [103]. In addition, there were some AD-associated proteins that show minor rescue levels, for example, Ncstn (-6%). Finally, in both the down- and the up-regulated proteins, some didn't change or dys-regulated further more by BNN27 (Supplementary Table S3).

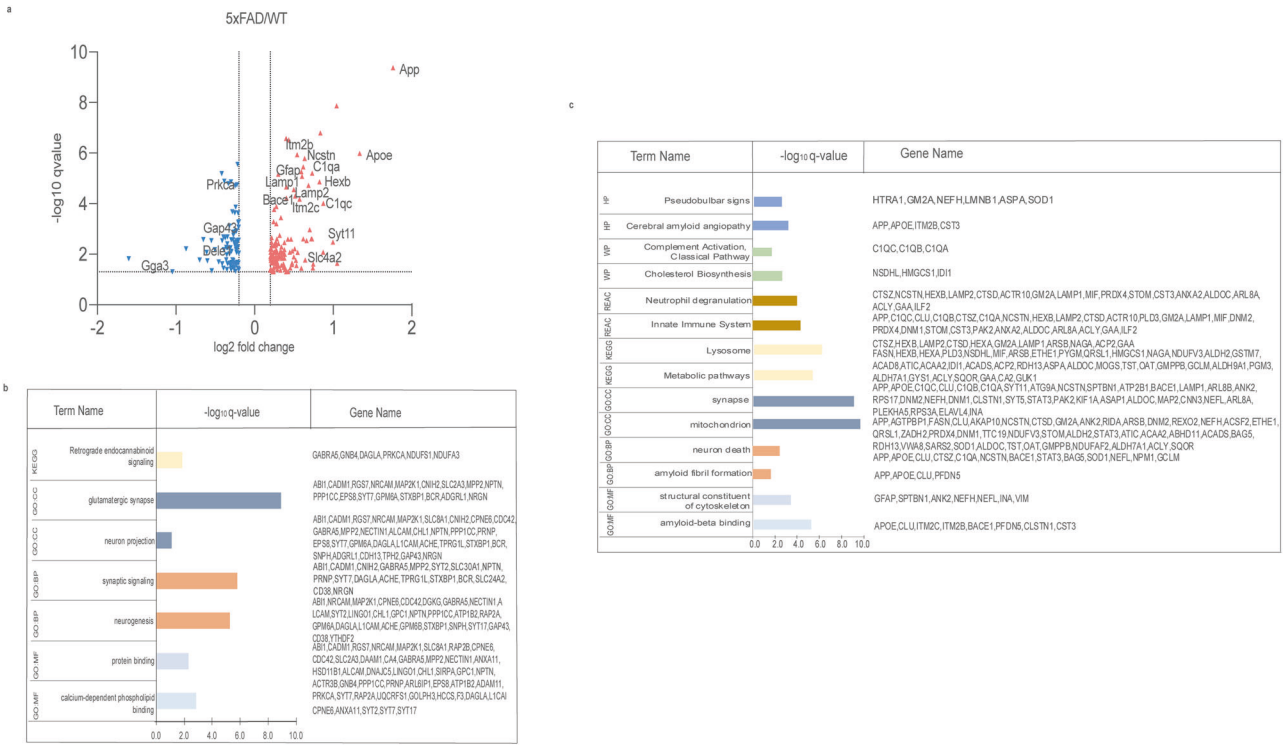

Fig. 7 Proteomics analysis shows the Aβ induced negative impact in 5xFAD mice. a Significantly regulated proteins in 5xFAD/WT comparison (FDR≤ 0.05, log2 fold change ≤ −0.2 or ≥0.2, pink: up-regulated, blue: down-regulated proteins), [**b**] protein group analysis on significantly down-regulated and [**c**] on significantly up-regulated proteins in the 5xFAD/WT comparison (enrichment analysis using the whole mouse genome as background).

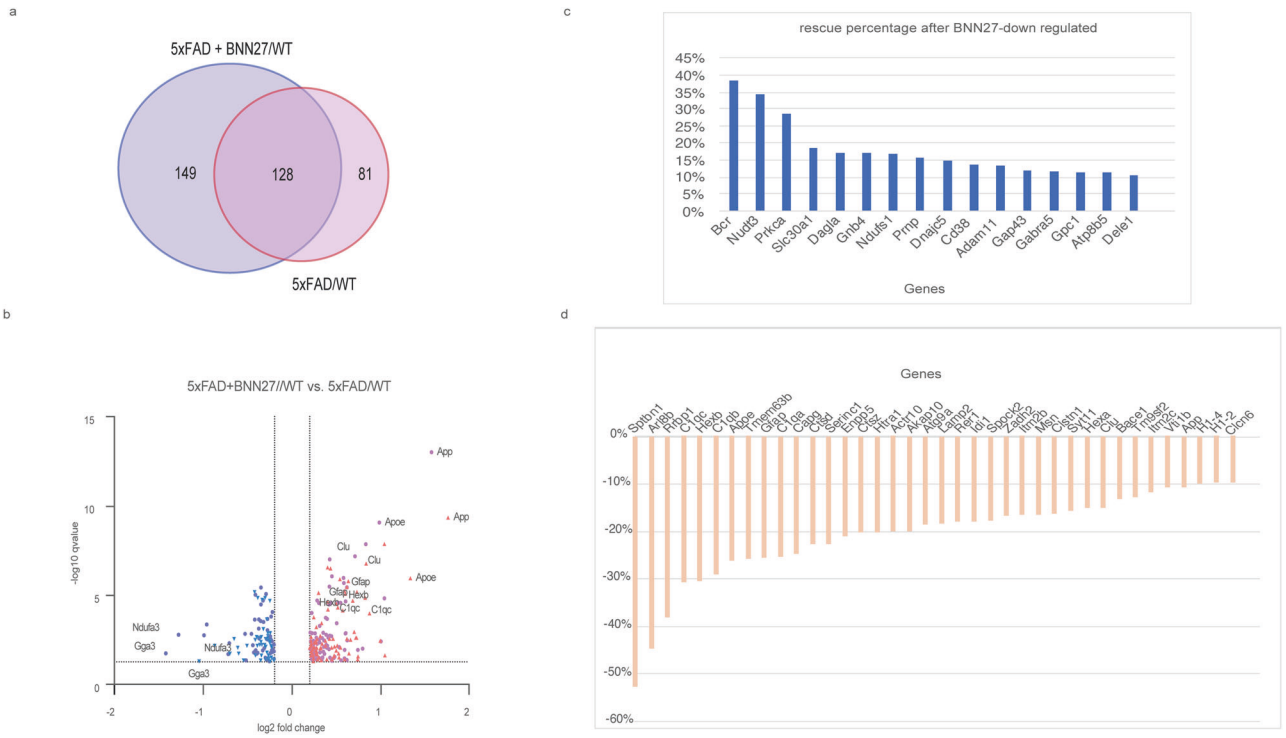

Fig. 8 Proteomics analysis shows that BNN27 has global rescue effects on Aβ induced negative impact in 5xFAD mice. a Venn diagram showing the common proteins that are present in both the 5xFAD+BNN27/WT and 5xFAD/WT comparisons, [**b**] double volcano blot showing the shift in log2 fold change induced by BNN27 (circle: 5xFAD+BNN27/WT, triangle:5xFAD/WT), [**c**] all rescued down- (≥10%) and [**d**] all up- (≤ −10%) rescued regulated proteins in 5xFAD+BNN27/WT compared with 5xFAD/WT shows the rescue effect in fold changes of major AD-induced proteins, in the presence of BNN27 (increase/decrease percentage in log2 fold change of proteins significantly regulated in both sets FDR ≤ 0.05, log2 fold change ≤ −0.2 or ≥0.2).

DISCUSSION

Neurotrophic factors are considered among the most important molecules for the development, maintenance and repair of vertebrate nervous system. Major challenges of the normally functioning neuronal cells consist the ageing and the neurodegeneration, where both significantly eliminate neurotrophin levels and thus exacerbate their deleterious effects, resulting in cognitive impairments and other severe, even life-threatening, pathologies. Noticeably, the most vulnerable and affected neuronal area in AD is the cholinergic pathway of basal forebrain [4, 9], that consists the only brain region that expresses both the high- and the low-affinity Nerve Growth Factor (NGF) receptors, namely TrkA and p75NTR respectively. In particular, during AD onset and progression, there is strong association between the deregulation of NGF signaling and the appearance of major disease hallmarks, including Aβ deposition which initiates cholinergic degeneration [7, 28]. The NGF-TrkA receptor complex of the basal forebrain cholinergic neurons has been shown to be disturbed in multiple ways [10, 33]. Specifically, mature NGF processing is altered towards pro-NGF, concomitantly with reduced TrkA receptor levels and increased membrane-located p75NTR [31, 104], which in turn shifts the balance towards increased pro-NGF/$p75^{NTR}$ pro-apoptotic signaling. Additionally to TrkA deregulation, Aβ-induced p75NTR signaling in cholinergic circuitry [39, 105] supports the merging of two old hypotheses for the emergence of AD, the cholinergic and neurotrophic ones, as a novel therapeutic target [2, 8]. Presently, available drugs against AD (acetylcholinesterase inhibitors) are targeting the sustainment of cholinergic function but only offer modest symptomatic relief. It is therefore of utmost importance the discovery of so-called "multifactorial disease modifying" therapies or drugs that could repair multiple pathological aspects of the disease. Although, new drugs for AD have just approved, targeting Aβ accumulation, alas sparking controversy among experts. On the other hand, NGF biodelivery by means of intracerebrovetricular injections or AAV2-NGF gene therapy are also facing undesired side effects and lack of effectiveness in patients, in addition to their difficulties in clinical application [29, 30]. To bypass these limitations and offer novel therapeutic solutions that take advantage of the pleiotropic effects of neurotrophins, small molecules that are BBB-permeable, have good pharmacokinetic properties and can act as NGF-mimetics represent good candidates to counteract in many ways the harmful Aβ-induced phenotype presented in AD.

In the present study we provide strong evidence that such a small-sized, lipophilic NGF analog, BNN27, exerts significant in vivo protective/anti-amyloidogenic, anti-inflammatory and neurogenic effects in an established mouse model of AD, the 5xFAD mice. BNN27, has been previously shown to mimic NGF and potentiate neuronal survival through the selective activation of TrkA [55] or $p75^{NTR}$ [56]. We now decipher its mechanism of action using primary neuronal populations of mature neurons and astrocytes, as well as neuronal precursors like NSCs and OPCs, challenged with the toxic oligomeric Aβ42 fibrils. More importantly, all these cellular actions of BNN27 were fully sufficient to provide a significant prevention of cognitive decline. Specifically, BNN27 could successfully diminish the harmful Aβ-induced effects such as cholinergic shrinkage-dysfunction restoring ChAT activity, synapse degeneration and neuroinflammation, as well as reduction of adult hippocampal neurogenesis, thus defining a pleiotropic mode of preventive action for this molecule. Experiments in primary hippocampal cultures under Aβ exposure that resemble the early and late onset of AD-dependent neuronal loss, revealed that this compound had strong effect in preventing and/or partially reversing neuronal cell death in all stages of degeneration. It is of particular interest that the protective effects of BNN27 in hippocampal neurons was mainly mediated through p75NTR. This pro-survival role of p75NTR upon its activation by BNN27 was also surprisingly revealed in granule cells of cerebellum [56], since BNN27 presents differential conformational interactions with neurotrophin receptors compared to the endogenous ligand, NGF. The p75NTR is suggested to have an enabling role in AD as it allows or enhances Aβ-induced toxicity in different AD models, is expressed by neurons known to degenerate in AD, including basal forebrain cholinergic, entorhinal, hippocampal, and cortical neurons, and its expression is increased in the AD brain [104]. BNN27 not only induces p75NTR down-regulation as we observed in this study (without affecting the TrkA levels), but additionally activates the receptor towards protective signals, such as the recruitment of TRAF6 which has been correlated to NFkB activation, promoting survival [106]. Additionally, there are in vitro indications that although p75NTR is providing neuroprotection against Amyloid-β in hippocampal neurons, its synergy with the Trk receptors upon BNN27 treatment is magnifying the neuroprotective effect.

Our aim was to investigate the role of neurotrophin analogs not only as neuroprotective factors but also as neurogenic compounds. Adult hippocampal neurogenesis (AHN) defines the generation of new neurons from adult neural progenitor cells in the dentate gyrus of the hippocampus throughout life. A plethora of recent research findings implicate adult hippocampal neurogenesis in memory performance, both in mice and humans [16, 17, 107]. Adult neurogenesis in the DG is a dynamic process that continuously reshapes the hippocampal formation and is important for neuroplasticity, learning and memory performance. Although, it is well documented that hippocampus and its DG are primarily affected in AD, and Aβ toxicity impairs adult neurogenesis [108], the molecular mechanisms connecting hippocampal neurogenesis and the underlying progressive memory loss in AD are poorly understood. A recent study by Dr Salta group [109] have shown that restoring adult neurogenesis through miR-132 was sufficient to improve memory in AD, while other results from Zhang et al (2021) [110, 111] proposed that modulation of adult neurogenesis have distinct impact on AD improvement.

Adult neurogenesis is altered in all animal models of Alzheimer's disease [112], mostly decreased, as well as in humans [113]. Neurotrophins, and especially BDNF, play an important regulatory role in adult neurogenesis as presented in a review by Vilar & Mira (2016) [114]. The p75NTR receptor also regulates hippocampal neurogenesis [115]. In our study, by measuring the DG-related neurogenesis in 5xFAD mice, we found that proliferation of Neural Stem Cells (NSCs) is reduced. Administration of BNN27 increased the number of BrdU-positive cells, while propagated their differentiation towards a neuronal cell type, in agreement with previous findings showing similar effects of NGF in NSCs [42]. Most importantly, isolated NSCs from the adult hippocampus that were cultured in vitro and challenged with different concentrations of Aβ, were rescued in the presence of 100 ng/ml of BNN27, an effect that seems to be dependent on both NGF receptors, TrkA and p75NTR. Since adult hippocampal neurogenesis is impaired in AD, it is assumed that this impairment compromises hippocampal function, representing a critical contributing factor to cognitive dysfunction in AD. Thus, BNN27 treatment could raise the possibility of stimulating inherent neurogenesis in our humanized mouse model, and might replace neurons lost and facilitate neuronal recovery and delay learning and memory impairment from the disease. An interesting finding is that BNN27 is reducing pro-inflammatory (A1) activation of astrocytes upon their stimulation with Aβ and microglia extract, an effect that could be associated to BNN27 neurogenic potential as indicated in a very recent study which highlights the role of NGFR (p75NTR) as inducer of neurogenesis due to suppression of astrogliosis [116]. Based on these findings, in vivo studies using 5xFAD mice crossed with p75NTR-knock out and knock-in strains are under development, in order to further understand the role of this neurotrophin receptor in AD, emphasizing in adult neurogenesis.

Finally, in our study we performed proteomic analysis in order to uncover genetic signatures of wild type vs 5xFAD mice, treated with BNN27 or placebo. In our study, BNN27 administration rescues 54 out of 128 dys-regulated proteins. Of particular interest is the rescue of the up-regulated Apoe and Tmem106b and of the down-regulated Adam11, among others. Apoe is a key player in the development of AD, by assisting the transport of cholesterol and other lipids in the bloodstream. The Apoe e4 allele is a well-established genetic risk factor and is associated with an increased risk of Aβ accumulation and inflammatory response of the brain. The rescue of Apoe in our model may imply the rescue of this specific allele, an emerging therapeutic target of AD [117, 118]. Transmembrane Protein 106B (Tmem106b), a lysosomal/endosomal protein has been of great interest lately, as it has been shown to form amyloid filaments in the aged human brain [119–121]. Lastly, the rescue of Adam metallopeptidase domain 11 (Adam11) is of interest due to its potential role in the pathophysiology of AD [122]. Research suggests that Adam11, like other proteins of the Adam family might play a role in the processing of amyloid precursor protein (App), which is involved in the generation of beta-amyloid, a key component of plaques in Alzheimer's disease, which is in accordance with our histopathological findings, pointing out the reduction of Aβ plaques upon BNN27 administration in the 5xFAD mice [123]. The proteomic results confirm that Aβ -induced pathology in the humanized mouse model of AD impairs major amyloidogenic and inflammatory pathways, while BNN27 treatment has restorative effects in several of them. Further analysis is needed in order to clarify the necessity of these pathways in neurotrophin-mediated effects in AD. Especially, in new components of the AD phenotype, such as oligodendrocytes and myelin, which seem not only to be affected by the disease, but also to drive specific pathologies [14]. Our results in the present study did not show significant differences on genotype and treatment, however BNN27 induced OPCs proliferation in vitro and previous study have shown its remyelinating ability in demyelination mouse models [58].

In conclusion, we have now described the multimodal in vivo effects of BNN27, a small molecule DHEA-derivative, which acts as a NGF mimetic exerting strong neuroprotective, anti-inflammatory, synaptogenic and neurogenic properties in the 5xFAD mouse model, and we have further determined its mechanism of actions against Aβ toxicity in in vitro hippocampal neurons and neural stem cell cultures. We aim to confirm these results of BNN27 in human induced Pluripotent Stem Cell (hiPSC)-derived neurons, originated from healthy and AD patients, in order to maximize its translational value as a lead compound with useful therapeutic properties against Alzheimer's Disease. Noticeably, the use of hiPSC models that resemble the main pathologies of AD have emerged the last years [124–126] and recent studies reveal the potential of small molecules with neurotrophic activity to protect iPSC-derived neurons [127], while our recent study has characterized a novel TrkB agonist as a strong neurogenic and neuroprotective agent using hiPSC models of AD [128]. At the present, we test BNN27 neurotrophic and anti-inflammatory activity in AD-derived hiPSC neuron and glial cultures, in order to confirm the mouse study and translate its potential to human cell systems, thus provide a lead molecule for pharmacological evaluation and therapeutic exploitation.

DATA AVAILABILITY

All materials are available upon request. Synthetic compounds are available under a Material Transfer Agreement with the University of Crete, FORTH and National Hellenic Research Foundation. The mass spectrometry proteomics datasets generated during the current study are available in the PRIDE repository, with the identifier PXD044699.

REFERENCES

1. World Alzheimer Report 2022: The Global Economic Impact of Dementia. London, UK: Alzheimer's Disease International.
2. Long JM, Holtzman DM. Alzheimer disease: an update on pathobiology and treatment strategies. Cell. 2019;179:312–39.
3. Wilson DM 3rd, Cookson MR, Van Den Bosch L, Zetterberg H, Holtzman DM, Dewachter I. Hallmarks of neurodegenerative diseases. Cell. 2023;186:693–714.
4. Coyle JT, Price DL, DeLong MR. Alzheimer's disease: a disorder of cortical cholinergic innervation. Science. 1983;219:1184–90.
5. Arendt T, Bigl V, Tennstedt A, Arendt A. Correlation between cortical plaque count and neuronal loss in the nucleus basalis in Alzheimer's disease. Neuroscience Letters. 1984;48:81–85.
6. Arendt T, Bigl V, Tennstedt A, Arendt A. Neuronal loss in different parts of the nucleus basalis is related to neuritic plaque formation in cortical target areas in Alzheimer's disease. Neuroscience. 1985;14:1–14.
7. Beach TG, Kuo Y-M, Spiegel K, Emmerling MR, Sue LI, Kokjohn K, et al. The cholinergic deficit coincides with Aβ deposition at the earliest histopathologic stages of Alzheimer disease. J Neuropathol Exp Neurol. 2000;59:308–13.
8. Hampel H, Mesulam M-M, Cuello AC, Farlow MR, Giacobini E, Grossberg GT, et al. The cholinergic system in the pathophysiology and treatment of Alzheimer's disease. Brain. 2018;141:1917–33.
9. Grothe M, Heinsen H, Teipel SJ. Atrophy of the cholinergic basal forebrain over the adult age range and in early stages of Alzheimer's disease. Biol Psychiatry. 2012;71:805–13.
10. De Strooper B, Karran E. The cellular phase of Alzheimer's disease. Cell. 2016;164:603–15.
11. DeKosky ST, Scheff SW. Synapse loss in frontal cortex biopsies in Alzheimer's disease: correlation with cognitive severity. Ann Neurol. 1990;27:457–64.
12. Gjoneska E, Pfenning AR, Mathys H, Quon G, Kundaje A, Tsai LH, et al. Conserved epigenomic signals in mice and humans reveal immune basis of Alzheimer's disease. Nature. 2015;518:365–9.
13. Heneka MT, Carson MJ, El Khoury J, Landreth GE, Brosseron F, Feinstein DL, et al. Neuroinflammation in Alzheimer's disease. In: The Lancet Neurology. 2015;14:388-405. NIH Public Access.
14. Depp C, Sun T, Sasmita AO, Spieth L, Berghoff SA, Nazarenko T, et al. Myelin dysfunction drives amyloid-β deposition in models of Alzheimer's disease. Nature. 2023;618:349–57.
15. Blanchard JW, Akay LA, Davila-Velderrain J, von Maydell D, Mathys H, Davidson SM, et al. APOE4 impairs myelination via cholesterol dysregulation in oligodendrocytes. Nature. 2022;611:769–79.
16. Choi SH, Tanzi RE. Adult neurogenesis in Alzheimer's disease. Hippocampus. 2023;33:307–21.
17. Moreno-Jiménez EP, Flor-García M, Terreros-Roncal J, Rábano A, Cafini F, Pallas-Bazarra N, et al. Adult hippocampal neurogenesis is abundant in neurologically healthy subjects and drops sharply in patients with Alzheimer's disease. Nat Med. 2019;25:554–60.
18. Salta E, Lazarov O, Fitzsimons CP, Tanzi R, Lucassen PJ, Choi SH. Adult hippocampal neurogenesis in Alzheimer's disease: A roadmap to clinical relevance. Cell Stem Cell. 2023;30:120–36.
19. Salloway S, Chalkias S, Barkhof F, Burkett P, Barakos J, Purcell D, et al. Amyloid-related imaging abnormalities in 2 phase 3 studies evaluating aducanumab in patients with early Alzheimer disease. JAMA Neurol. 2022;79:13–21.
20. Cummings JL, Morstorf T, Zhong K. Alzheimer's disease drug-development pipeline: few candidates, frequent failures. Alzheimers Res. Ther. 2014;6:37.
21. Ebell MH, Barry HC. Why physicians should not prescribe aducanumab for Alzheimer disease. Am. Fam. Physician. 2022;105:353–4.
22. van Dyck CH, Swanson CJ, Aisen P, Bateman RJ, Chen C, Gee M, et al. Lecanemab in early Alzheimer's disease. N Engl J Med. 2023;388:9–21.
23. Huang EJ, Reichardt LF. Neurotrophins: roles in neuronal development and function. Annu Rev Neurosci. 2001;24:677–736.
24. Chao MV. Neurotrophins and their receptors: a convergence point for many signalling pathways. Nat Rev Neurosci. 2003;4:299–309.
25. Meldolesi J. Neurotrophin receptors in the pathogenesis, diagnosis and therapy of neurodegenerative diseases. Pharmacol Res. 2017;121:129–37.
26. Dechant G, Barde YA. The neurotrophin receptor p75(NTR): novel functions and implications for diseases of the nervous system. Nat Neurosci. 2002;5:1131–6.
27. Levi-Montalcini R, Booker B. Destruction of the sympathetic ganglia in mammals by an antiserum to a nerve-growth protein. Proc. Natl. Acad. Sci. 1960;46:384–91.
28. Mufson EJ, Counts SE, Ginsberg SD, Mahady L, Perez SE, Massa SM, et al. Nerve growth factor pathobiology during the progression of Alzheimer's disease. Front Neurosci. 2019;13:533.
29. Tuszynski MH, Thal L, Pay M, Salmon DP, Bakay R, Patel P, et al. A phase 1 clinical trial of nerve growth factor gene therapy for Alzheimer disease. Nat Med. 2005;11:551–5.

30. Rafii MS, Baumann TL, Bakay RA, Ostrove JM, Siffert J, Fleisher AS, et al. A phase 1 study of stereotactic gene delivery of AAV2-NGF for Alzheimer's disease. Alzheimers Dement. 2014;10:571–81.
31. Capsoni S, Tiveron C, Vignone D, Amato G, Cattaneo A. Dissecting the involvement of tropomyosin-related kinase A and p75 neurotrophin receptor signaling in NGF deficit-induced neurodegeneration. Proc Natl Acad Sci USA. 2010;107:12299–304.
32. Ginsberg SD, Malek-Ahmadi MH, Alldred MJ, Che S, Elarova I, Chen Y, et al. Selective decline of neurotrophin and neurotrophin receptor genes within CA1 pyramidal neurons and hippocampus proper: Correlation with cognitive performance and neuropathology in mild cognitive impairment and Alzheimer's disease. Hippocampus. 2019;29:422–39.
33. Hefti F, Will B. Nerve growth factor is a neurotrophic factor for forebrain cholinergic neurons; implications for Alzheimer's disease. J Neural Transm Suppl. 1987;24:309–15.
34. Sanchez-Ortiz E, Yui D, Song D, Li Y, Rubenstein JL, Reichardt LF, et al. TrkA gene ablation in basal forebrain results in dysfunction of the cholinergic circuitry. J Neurosci. 2012;32:4065–79.
35. Demuth H, Hosseini S, Düsedeau HP, Dunay IR, Korte M, Zagrebelsky M. Deletion of p75NTR rescues the synaptic but not the inflammatory status in the brain of a mouse model for Alzheimer's disease. Front Mol Neurosci. 2023;16:1163087.
36. Qian L, Milne MR, Shepheard S, Rogers ML, Medeiros R, Coulson EJ. Removal of p75 neurotrophin receptor expression from cholinergic basal forebrain neurons reduces amyloid-β plaque deposition and cognitive impairment in aged APP/PS1 mice. Mol Neurobiol. 2019;56:4639–52. https://doi.org/10.1007/s12035-018-1404-2.
37. Knowles JK, Rajadas J, Nguyen TV, Yang T, LeMieux MC, Vander Griend L, et al. The p75 neurotrophin receptor promotes amyloid-beta (1-42)-induced neuritic dystrophy in vitro and in vivo. J Neurosci. 2009;29:10627–37.
38. Perini G, Della-Bianca V, Politi V, Della Valle G, Dal-Pra I, Rossi F, et al. Role of p75 neurotrophin receptor in the neurotoxicity by beta-amyloid peptides and synergistic effect of inflammatory cytokines. J Exp Med. 2002;195:907–18.
39. Yaar M, Zhai S, Pilch PF, Doyle SM, Eisenhauer PB, et al. Binding of beta-amyloid to the p75 neurotrophin receptor induces apoptosis. A possible mechanism for Alzheimer's disease. J Clin Invest. 1997;100:2333–40.
40. Rabizadeh S, Bitler CM, Butcher LL, Bredesen DE. Expression of the low-affinity nerve growth factor receptor enhances beta-amyloid peptide toxicity. Proc Natl Acad Sci USA. 1994;91:10703–6.
41. Shanks HRC, Chen K, Reiman EM, Blennow K, Cummings JL, Massa SM, et al. p75 neurotrophin receptor modulation in mild to moderate Alzheimer disease: a randomized, placebo-controlled phase 2a trial. Nat Med. 2024;30:1761–70.
42. Frielingsdorf H, Simpson DR, Thal LJ, Pizzo DP. Nerve growth factor promotes survival of new neurons in the adult hippocampus. Neurobiol Dis. 2007;26:47–55.
43. Mitra S, Gera R, Linderoth B, Lind G, Wahlberg L, Almqvist P, et al. Review of techniques for biodelivery of nerve growth factor (NGF) to the brain in relation to Alzheimer's disease. Adv Exp Med Biol. 2021;1331:167–91.
44. Capsoni S, Marinelli S, Ceci M, Vignone D, Amato G, Malerba F, et al. Intranasal "painless" human Nerve Growth Factor slows amyloid neurodegeneration and prevents memory deficits in App X PS1 mice. PLoS One. 2012;7:e37555.
45. Longo FM, Massa SM. Small-molecule modulation of neurotrophin receptors: a strategy for the treatment of neurological disease. Nat Rev Drug Discov. 2013;12:507–25.
46. Kazim SF, Iqbal K. Neurotrophic factor small-molecule mimetics mediated neuroregeneration and synaptic repair: emerging therapeutic modality for Alzheimer's disease. Mol Neurodegener. 2016;11:50.
47. Xhima K, Markham-Coultes K, Nedev H, Heinen S, Saragovi HU, Hynynen K, et al. Focused ultrasound delivery of a selective TrkA agonist rescues cholinergic function in a mouse model of Alzheimer's disease. Sci Adv. 2020;6:eaax6646.
48. Scarpi D, Cirelli D, Matrone C, Castronovo G, Rosini P, Occhiato EG, et al. Low molecular weight, non-peptidic agonists of TrkA receptor with NGF-mimetic activity. Cell Death Dis. 2012;3:e339.
49. Jang SW, Okada M, Sayeed I, Xiao G, Stein D, Jin P, et al. Gambogic amide, a selective agonist for TrkA receptor that possesses robust neurotrophic activity, prevents neuronal cell death. Proc Natl Acad Sci USA. 2007;104:16329–34.
50. Knowles JK, Simmons DA, Nguyen TV, Vander Griend L, Xie Y, Zhang H, et al. Small molecule p75NTR ligand prevents cognitive deficits and neurite degeneration in an Alzheimer's mouse model. Neurobiol Aging. 2013;34:2052–63.
51. Xie Y, Meeker RB, Massa SM, Longo FM. Modulation of the p75 neurotrophin receptor suppresses age-related basal forebrain cholinergic neuron degeneration. Sci Rep. 2019;9:5273.
52. Charalampopoulos I, Tsatsanis C, Dermitzaki E, Alexaki VI, Castanas E, Margioris AN, et al. Dehydroepiandrosterone and allopregnanolone protect sympathoadrenal medulla cells against apoptosis via antiapoptotic Bcl-2 proteins. Proc Natl Acad Sci USA. 2004;101:8209–14.
53. Lazaridis I, Charalampopoulos I, Alexaki VI, Avlonitis N, Pediaditakis I, et al. Neurosteroid dehydroepiandrosterone interacts with nerve growth factor (NGF) receptors, preventing neuronal apoptosis. PLoS Biol. 2011;9:e1001051.
54. Calogeropoulou T, Avlonitis N, Minas V, Alexi X, Pantzou A, Charalampopoulos I, et al. Novel dehydroepiandrosterone derivatives with antiapoptotic, neuroprotective activity. J Med Chem. 2009;52:6569–87.
55. Pediaditakis I, Efstathopoulos P, Prousis KC, Zervou M, Arévalo JC, Alexaki VI, et al. Selective and differential interactions of BNN27, a novel C17-spiroepoxy steroid derivative, with TrkA receptors, regulating neuronal survival and differentiation. Neuropharmacology. 2016;111:266–82.
56. Pediaditakis I, Kourgiantaki A, Prousis KC, Potamitis C, Xanthopoulos KP, Zervou M, et al. BNN27, a 17-Spiroepoxy Steroid Derivative, Interacts With and Activates p75 Neurotrophin Receptor, Rescuing Cerebellar Granule Neurons from Apoptosis. Front Pharmacol. 2016;7:512.
57. Ibán-Arias R, Lisa S, Mastrodimou N, Kokona D, Koulakis E, Iordanidou P, et al. The synthetic microneurotrophin BNN27 affects retinal function in rats with streptozotocin-induced diabetes. Diabetes. 2018;67:321–33.
58. Bonetto G, Charalampopoulos I, Gravanis A, Karagogeos D. The novel synthetic microneurotrophin BNN27 protects mature oligodendrocytes against cuprizone-induced death, through the NGF receptor TrkA. GLIA. 2017;65:1376–94.
59. Pitsikas N, Zoupa E, Gravanis A. The novel dehydroepiandrosterone (DHEA) derivative BNN27 counteracts cognitive deficits induced by the D1/D2 dopaminergic receptor agonist apomorphine in rats. Psychopharmacology (Berl). 2021;238:227–37.
60. Georgelou K, Saridaki EA, Karali K, Papagiannaki A, Charalampopoulos I, Gravanis A, et al. Microneurotrophin BNN27 reduces astrogliosis and increases density of neurons and implanted neural stem cell-derived cells after spinal cord injury. Biomedicines. 2023;11:1170.
61. Ibán-Arias R, Lisa S, Poulaki S, Mastrodimou N, Charalampopoulos I, Gravanis A, et al. Effect of topical administration of the microneurotrophin BNN27 in the diabetic rat retina. Graefes Arch Clin Exp Ophthalmol. 2019;257:2429–36.
62. Oakley H, Cole SL, Logan S, Maus E, Shao P, Craft J, et al. Intraneuronal β-amyloid aggregates, neurodegeneration, and neuron loss in transgenic mice with five familial Alzheimer's disease mutations: Potential factors in amyloid plaque formation. J. Neurosci. 2006;26:10129–40.
63. Tsika C, Tzatzarakis MN, Antimisiaris SG, Tsoka P, Efstathopoulos P, Charalampopoulos I, et al. Quantification of BNN27, a novel neuroprotective 17-spiroepoxy dehydroepiandrosterone derivative in the blood and retina of rodents, after single intraperitoneal administration. Pharmacol Res Perspect. 2021;9:e00724.
64. Deacon RM, Rawlins JN. T-maze alternation in the rodent. Nat Protoc. 2006;1:7–12.
65. Franklin KBJ, Paxinos G The mouse brain in stereotaxic coordinates. San Diego; London: Academic Press. 1997.
66. Li W, Poteet E, Xie L, Liu R, Wen Y, Yang SH. Regulation of matrix metalloproteinase 2 by oligomeric amyloid β protein. Brain Research. 2011;1387:141–8.
67. Efstathopoulos P, Kourgiantaki A, Karali K, Sidiropoulou K, Margioris AN, Gravanis A, et al. Fingolimod induces neurogenesis in adult mouse hippocampus and improves contextual fear memory. Transl Psychiatry. 2015;5.
68. Beaudoin GM 3rd, Lee SH, Singh D, Yuan Y, Ng YG, Reichardt LF, et al. Culturing pyramidal neurons from the early postnatal mouse hippocampus and cortex. Nat Protoc. 2012;7:1741–54.
69. Solà C, Cristòfol R, Suñol C, Sanfeliu C. Primary cultures for neurotoxicity testing. In: Cell Culture Techniques. 2011; (Aschner, M et al., eds), pp 87-103 Totowa, NJ: Humana Press.
70. Saura J, Tusell JM, Serratosa J. High-yield isolation of murine microglia by mild trypsinization. GLIA. 2003;44:183–9.
71. McCarthy KD, de Vellis J. Preparation of separate astroglial and oligodendroglial cell cultures from rat cerebral tissue. J Cell Biol. 1980;85:890–902.
72. Tamashiro TT, Dalgard CL, Byrnes KR. Primary microglia isolation from mixed glial cell cultures of neonatal rat brain tissue. J Vis Exp. 2012:e3814.
73. Van der Spek SJF, Koopmans F, Paliukhovich I, Ramsden SL, Harvey K. Harvey, et al. Glycine Receptor Complex Analysis Using Immunoprecipitation-Blue Native Gel Electrophoresis-Mass Spectrometry. Proteomics. 2020;20:e1900403.
74. Li KW, Chen N, Klemmer P, Koopmans F, Karupothula R, Smit AB. Identifying true protein complex constituents in interaction proteomics: The example of the DMXL2 protein complex. Proteomics. 2012;12:2428–32.
75. Koopmans F, Pandya NJ, Franke SK, Phillippens I, Paliukhovich I, Li KW, et al. Comparative hippocampal synaptic proteomes of rodents and primates: differences in neuroplasticity-related proteins. Frontiers in molecular neuroscience. 2018;11:364.
76. Koopmans F, Li KW, Klaassen RV, Smit AB. MS-DAP platform for downstream data analysis of label-free proteomics uncovers optimal workflows in

benchmark data sets and increased sensitivity in analysis of Alzheimer's biomarker data. J. Proteome Res. 2022;22:374–86.
77. Perez-Riverol Y, Bai J, Bandla C, Garcia-Seisdedos D, Hewapathirana S, Kamatchinathan S, et al. The PRIDE database resources in 2022: A hub for mass spectrometry-based proteomics evidences. Nucleic Acids. Res. 2022;50:D543–D552.
78. Knierim JJ. The hippocampus. Curr Biol CB. 2015;25:R1116–1121.
79. Kwon HS, Koh SH. Neuroinflammation in neurodegenerative disorders: the roles of microglia and astrocytes. Transl Neurodegener. 2020;9:42.
80. Hsiao K, Chapman P, Nilsen S, Eckman C, Harigaya Y, Younkin S, et al. Correlative memory deficits, Aβ elevation, and amyloid plaques in transgenic mice. Science. 1996;274:99–102.
81. Sturchler-Pierrat C, Abramowski D, Duke M, Wiederhold KH, Mistl C, Rothacher S, et al. Two amyloid precursor protein transgenic mouse models with Alzheimer disease-like pathology. Proc Natl Acad Sci USA. 1997;94:13287–92.
82. Yan H, Pang P, Chen W, Zhu H, Henok KA, Li H, et al. the lesion analysis of cholinergic neurons in 5XFAD mouse model in the three-dimensional level of whole brain. Molecular Neurobiology. 2018;55:4115–25.
83. Miller DL, Papayannopoulos IA, Styles J, Bobin SA, Lin YY, Biemann K, et al. Peptide compositions of the cerebrovascular and senile plaque core amyloid deposits of Alzheimer's disease. Arch Biochem Biophys. 1993;301:41–52.
84. Bitan G, Kirkitadze MD, Lomakin A, Vollers SS, Benedek GB, Teplow DB. Amyloid beta -protein (Abeta) assembly: Abeta 40 and Abeta 42 oligomerize through distinct pathways. Proc Natl Acad Sci USA. 2003;100:330–5.
85. Serrano-Pozo A, Muzikansky A, Gomez-Isla T, Growdon JH, Betensky RA, Frosch MP, et al. Differential relationships of reactive astrocytes and microglia to fibrillar amyloid deposits in Alzheimer disease. J Neuropathol Exp Neurol. 2013;72:462–71.
86. Kaech S, Banker G. Culturing hippocampal neurons. Nat Protoc. 2006;1:2406–15.
87. Crowley LC, Waterhouse NJ. Detecting Cleaved Caspase-3 in Apoptotic Cells by Flow Cytometry. Cold Spring Harb Protoc. 2016;2016.
88. van Dijk MT, Fenton AA. On how the dentate gyrus contributes to memory discrimination. Neuron. 2018;98:832–845.e5.
89. Gage FH. Mammalian neural stem cells. Science. 2000;287:1433–8.
90. Van Praag H, Schinder AF, Christle BR, Toni N, Palmer TD, Gage FH. Functional neurogenesis in the adult hippocampus. Nature. 2002;415:1030–4.
91. Krishnasamy S, Weng YC, Thammisetty SS, Phaneuf D, Lalancette-Hebert M, Kriz J. Molecular imaging of nestin in neuroinflammatory conditions reveals marked signal induction in activated microglia. J Neuroinflammation. 2017;14:45.
92. Sierksma A, Lu A, Mancuso R, Fattorelli N, Thrupp N, Salta E, et al. Novel Alzheimer risk genes determine the microglia response to amyloid-beta but not to TAU pathology. EMBO Mol. Med. 2020;12:e10606.
93. Sakurai T, Kaneko K, Okuno M, Wada K, Kashiyama T, Shimizu H, et al. Membrane microdomain switching: a regulatory mechanism of amyloid precursor protein processing. J Cell Biol. 2008;183:339–52.
94. Zhao J, Liu X, Xia W, Zhang Y, Wang C. Targeting amyloidogenic processing of APP in Alzheimer's disease. Front. Mol. Neurosci. 2020;13:137.
95. Mi S, Miller RH, Lee X, Scott ML, Shulag-Morskaya S, Shao Z, et al. LINGO-1 negatively regulates myelination by oligodendrocytes. Nat Neurosci. 2005;8:745–51.
96. Zolochevska O, Bjorklund N, Woltjer R, Wiktorowicz JE, Taglialatela G. Postsynaptic Proteome of Non-Demented Individuals with Alzheimer's Disease Neuropathology. J Alzheimers Dis. 2018;65:659–82.
97. Gentile MT, Reccia MG, Sorrentino PP, Vitale E, Sorrentino G, Puca AA, et al. Role of cytosolic calcium-dependent phospholipase A2 in Alzheimer's disease pathogenesis. Mol Neurobiol. 2012;45:596–604.
98. Recuero M, Vicente MC, Martínez-García A, Ramos MC, Carmona-Saez P, Sastre I, et al. A free radical-generating system induces the cholesterol biosynthesis pathway: a role in Alzheimer's disease. Aging Cell. 2009;8:128–39.
99. Boeddrich A, Haenig C, Neuendorf N, Blanc E, Ivanov A, Kirchner M, et al. Proteomics analysis of 5xFAD mouse brain regions reveals the lysosome-associated protein Arl8b as a candidate biomarker for Alzheimer's disease. Genome Med. 2023;15:50.
100. Coskuner O, Murray IVJ. Adenosine triphosphate (ATP) reduces amyloid-β protein misfolding in vitro. J Alzheimers Dis. 2014;41:561–74.
101. Bainbridge MN, Mazumder A, Ogasawara D, Jamra RA, Bernard G, Bertini E, et al. Endocannabinoid dysfunction in neurological disease: neuro-ocular DAGLA-related syndrome. Brain. 2022;145:3383–90.
102. Cuervo A, Wong E. Chaperone-mediated autophagy: roles in disease and aging. Cell Res. 2014;24:92–104.
103. Stilling RM, Benito E, Gertig M, Barth J, Capece V, Burkhardt S, et al. De-regulation of gene expression and alternative splicing affects distinct cellular pathways in the aging hippocampus. Front Cell Neurosci. 2014;13:373.
104. Chakravarthy B, Menard M, Ito S, Gaudet C, Dal Pra I, Armato U, et al. Hippocampal membrane-associated p75NTR levels are increased in Alzheimer's disease. J Alzheimers Dis. 2012;30:675–84.
105. Sotthibundhu A, Sykes AM, Fox B, Underwood CK, Thangnipon W, Coulson EJ. β-Amyloid1–42 Induces Neuronal Death through the p75 Neurotrophin Receptor. Journal of Neuroscience. 2008;28:3941–6.
106. Charalampopoulos I, Vicario A, Pediaditakis I, Gravanis A, Simi A, Ibáñez CF. Genetic dissection of neurotrophin signaling through the p75 neurotrophin receptor. Cell Rep. 2012;2:1563–70.
107. Babcock KR, Page JS, Fallon JR, Webb AE. Adult hippocampal neurogenesis in aging and Alzheimer's disease. Stem Cell Reports. 2021;16:681–93.
108. Sanila A, Sumera Mirza FJ, Asif M, Hasim D, Ahmed T, Zahid S. Amyloid-beta induced neurotoxicity impairs cognition and adult hippocampal neurogenesis in a mouse model for Alzheimer's disease. Curr Alzheimer Res. 2020;17:1033–42.
109. Walgrave H, Balusu S, Snoeck S, Vanden Eynden E, Craessaerts K, Thrupp N, et al. Restoring miR-132 expression rescues adult hippocampal neurogenesis and memory deficits in Alzheimer's disease. Cell Stem Cell. 2021;28:1805–1821.e8.
110. Zhang XQ, Mei YF, He Y, Wang DP, Wang J, Wei XJ, et al. Ablating adult neural stem cells improves synaptic and cognitive functions in Alzheimer models. Stem Cell. Rep. 2021;16:89–105.
111. Zhang X, Wei X, Mei Y, Wang D, Wang J, Zhang Y, et al. Modulating adult neurogenesis affects synaptic plasticity and cognitive functions in mouse models of Alzheimer's disease. Stem Cell Reports. 2021;16:3005–19.
112. Chuang TT. Neurogenesis in mouse models of Alzheimer's disease. Biochim Biophys Acta. 2010;1802:872–80.
113. Terreros-Roncal J, Moreno-Jiménez EP, Flor-García M, Rodríguez-Moreno CB, Trinchero MF, Cafini F, et al. Impact of neurodegenerative diseases on human adult hippocampal neurogenesis. Science. 2021;374:1106–13.
114. Vilar M, Mira H. Regulation of neurogenesis by neurotrophins during adulthood: expected and unexpected roles. Front Neurosci. 2016;10:26.
115. Catts VS, Al-Menhali N, Burne TH, Colditz MJ, Coulson EJ. The p75 neurotrophin receptor regulates hippocampal neurogenesis and related behaviours. Eur J Neurosci. 2008;28:883–92.
116. Siddiqui T, Cosacak MI, Popova S, Bhattarai P, Yilmaz E, Lee AJ, et al. Nerve growth factor receptor (Ngfr) induces neurogenic plasticity by suppressing reactive astroglial Lcn2/Slc22a17 signaling in Alzheimer's disease. NPJ Regen Med. 2023;8:33.
117. Lin YT, Seo J, Gao F, Feldman HM, Wen HL, Penney J, et al. APOE4 causes widespread molecular and cellular alterations associated with Alzheimer's disease phenotypes in human iPSC-derived brain cell types. Neuron. 2018;98:1141–1154.e7.
118. Victor MB, Leary N, Luna X, Meharena HS, Scannail AN, Bozzelli PL, et al. Lipid accumulation induced by APOE4 impairs microglial surveillance of neuronal-network activity. Cell Stem Cell. 2022;29:1197–1212.e8.
119. Schweighauser M, Arseni D, Bacioglu M, Huang M, Lovestam S, Shi Y, et al. Age-dependent formation of TMEM106B amyloid filaments in human brains. Nature. 2022;605:310–4.
120. Chang A, Xiang X, Wang J, Lee C, Arakhamia T, Simjanoska M, et al. Homotypic fibrillization of TMEM106B across diverse neurodegenerative diseases. Cell. 2022;185:1346–1355.e15.
121. Jiang YX, Cao Q, Sawaya MR, Abskharon R, Ge P. De Ture, et al. Amyloid fibrils in FTLD-TDP are composed of TMEM106B and not TDP-43. Nature. 2022;605:304–9.
122. Rybnikova E, Karkkainen I, Pelto-Huikko M, Huovila AP. Developmental regulation and neuronal expression of the cellular disintegrin ADAM11 gene in mouse nervous system. Neuroscience. 2002;112:921–34.
123. Yang Y, Tapias V, Acosta D, Xu H, Chen H, Bhawal R, et al. Altered succinylation of mitochondrial proteins, APP and tau in Alzheimer's disease. Nat Commun. 2022;13:159.
124. Grenier K, Kao J, Diamandis P. Three-dimensional modeling of human neurodegeneration: brain organoids coming of age. Mol Psychiatry. 2020;25:254–74.
125. Penney J, Ralvenius WT, Tsai LH. Modeling Alzheimer's disease with iPSC-derived brain cells. Mol Psychiatry. 2020;25:148–67.
126. De Rus Jacquet A, Denis HL, Cicchetti F, Alpaugh M. Current and future applications of induced pluripotent stem cell-based models to study pathological proteins in neurodegenerative disorders. Mol Psychiatry. 2021;26:2685–706.
127. Gonzalez S, McHugh TLM, Yang T, Syriani W, Massa SM, Longo FM, et al. Small molecule modulation of TrkB and TrkC neurotrophin receptors prevents cholinergic neuron atrophy in an Alzheimer's disease mouse model at an advanced pathological stage. Neurobiol Dis. 2022;162:105563.
128. Charou D, Rogdakis T, Latorrata A, Valcarcel M, Papadogiannis V, Athanasiou C, et al. Comprehensive characterization of the neurogenic and neuroprotective action of a novel TrkB agonist using mouse and human stem cell models of Alzheimer's disease. Stem Cell Res Ther. 2024;15:200.

ACKNOWLEDGEMENTS

We thank I. Pauliukovich for her help with mass spectrometry.

AUTHOR CONTRIBUTIONS

MK, KK, PE: in vivo experiments, in vitro experiments, analysis of results, first preparation of results, figures and graphs; Participation in writing manuscript and revisions. MK, MAP, ET, IZ, AT, TC: in vitro experiments, preparation of primary cells, analysis of study results, participation in conceptualization and writing draft manuscript. MK, KK, ET, KWL, KS, IC: data analysis, conceptualization and design of all experiments, writing of paper, supervision, funding; IC, AG: supervision, funding, writing manuscript.

FUNDING

This research was funded by: (1) DINNESMIN grant, co-financed by the European Regional Development Fund of the European Union and Greek national funds through the Operational Program Competitiveness, Entrepreneurship and Innovation (ΕΠΑΝΕΚ)' of the NSRF 2014-2020, under the call RESEARCH-CREATE-INNOVATE (project code: T1EDK-03186, Acronym: DINNESMIN) (KA10186), to Achille Gravanis and Ioannis Charalampopoulos (2) the Hellenic Foundation for Research and Innovation (H.F.R.I.) under the "1st Call for H.F.R.I. Research Projects to support Faculty members and Researchers and the procurement of high-cost research equipment" (Project Number: 2301, KA10490) to I. Charalampopoulos, (3) the European Union's Horizon 2020 research and innovation program "Euroneurotrophin" under the Marie Skłodowska-Curie grant agreement No. 765704, (4) the European Union HORIZON, under the European Innovation Council (EIC)-2022-PATHFINDEROPEN-01 program "SoftReach", No 101099145 and (5) co-financed by the national Flagship Action "Hellenic Precision Medicine Network in Neurodegenerative Diseases", funded by the Ministry of Development and Investment and the General Secretariat for Research and Innovation (GSRI).

COMPETING INTERESTS

All authors, except Achille Gravanis, declare that they have not any competing financial interests in relation to the work described. Dr Achille Gravanis is the co-founder of spin-off Bionature EA LTD, proprietary of compound BNN27 (patented with the WO 2008/ 1555 34 A2 number at the World Intellectual Property Organization). Gravanis A is co-founder of Bionature E.A. Ltd. The BNN compounds are proprietary and patented by the Bionature E.A. Ltd (http://www.bionature.net) (Patent Number: WO2008/155534 A2).

INSTITUTIONAL REVIEW BOARD STATEMENT

The study was conducted according to the guidelines of the Declaration of Helsinki, and approved by the Ethics Committee of FORTH (protocol code 262272 and date of approval 29 October 2018, FORTH Institute animal license: EL91-BIObr-01 and EL91-BIOexp-02). All primary cells derived from animals that were grouped housed in the Animal House of the Institute of Molecular Biology and Biotechnology (IMBB-FoRTH, Heraklion, Greece), in a temperature-controlled facility on a 12-h light/dark cycle, fed by standard chow diet and water ad libitum. All research activities strictly adhered to the EU adopted Directive 2010/63/EU on the protection of animals used for scientific purposes. All procedures were performed under the approval of Veterinary Directorate of Prefecture of Heraklion (Crete) and carried out in compliance with Greek Government guidelines and the guidelines of FORTH ethics committee and were performed in accordance with approved protocols from the Federation of European Laboratory Animal Science Associations (FELASA) and Use of Laboratory animals [License number: EL91-BIOexp-02), Approval Code: 360667, Approval Date: 29/11/2021 (active for 3 years)].

ADDITIONAL INFORMATION

Supplementary information The online version contains supplementary material available at https://doi.org/10.1038/s41380-024-02833-w.

Correspondence and requests for materials should be addressed to Ioannis Charalampopoulos.